

Dear Editor

Many thanks for handling our paper and for contacting several reviewers, who came back with critical, though constructive and helpful comments. We greatly acknowledge the feedbacks and suggestions of an additional comment, which we have fully considered upon revising our article. Many thanks for these contributions!

## **Outline of how we have addressed the major points raised by the reviewers**

The reviewers centered their critiques and concerns on three closely related issues, which we have not considered with the required care upon writing our first version of this manuscript. We addressed these points and thus took the opportunity to complement our manuscript with additional information to better constrain our inferences. The major points concern (i) the differences between threshold conditions for floods resulting in either an alteration of the channel architecture (channel forming floods) or in the incipient motion of individual clasts (A. Wickert); (ii) the importance of protrusion effects on the entrainment of large clasts and the consequences on the Shields variable  $\phi$  (A. Wickert; R. Hodges), and (iii) mismatches between experimental results and our inferences (P. Carling, R. Hodges, McLelland). We have addressed these points in three new individual chapters in the manuscript. There, we shortly summarize the related state of research, and we outline where these points contradict with our conclusions, and how. We then have adjusted our inferences and interpretations accordingly.

As a major outcome of our revision, we specified the conditions under which imbrications possibly record the occurrence of supercritical flows. In particular, we find that *imbrications possibly record supercritical flows provided that (i)  $\phi$ -values are larger than c. 0.05, which might be appropriate for streams in the Swiss Alps; (ii) average stream gradients exceed c.  $0.5 \pm 0.1^\circ$ ; and that (iii) relative bed roughness values, i.e. the ratio between the water depth  $d$  and the  $D_{84}$ , are larger than  $-0.06 \pm 0.01$ . While we cannot rule out that imbrication may be formed during subcritical flows with  $\phi$ -values as low as 0.03, as a large number of flume experiments reveal, our results from Alpine streams suggest that clast imbrications are likely recorders of upper flow regime conditions, provided that the clasts form well-sorted and densely packed clusters. We consider that these differences may be rooted in a misfit between the observational and experimental scales. (please see lines in the revised manuscript 24-33).*

As a consequence, we changed the title to *Clast imbrications in coarse-grained mountainous streams and stratigraphic archives possibly suggest deposition under upper flow regime conditions.*

Please find below a summary of how we have addressed the major points (i) to (iii).

### **Differences between thresholds for sediment transport during channel forming floods and during the incipient motion of individual clasts**

We have discussed this point in a separate section, where we outlined (i) why this distinction will not change our major conclusions, and (ii) why the consideration of the incipient motion of individual clasts is a more appropriate approach for the understanding of imbrication formation. We mention that our calculations are based on the incipient motion of individual clasts, which we use as justification for selection of equation (1a) for all other considerations. *This approach might be perceived as a large contrast to the hydrological conditions during channel forming floods where thresholds for the evacuation of sediment are up to 1.2 times larger, as theoretical and field-based analyses and have shown (Parker, 1978; Philips and Jerolmack, 2016; Pfeiffer et al., 2017). Nevertheless, the consequences on the outcome of our calculations are minor, at least when the Froude number dependencies on the slope and bed roughness parameters are considered. In fact, a 1.2-times larger threshold will increase the  $\phi$ -values (equation 1b) to the range between*

0.036 and 0.072. However, as illustrated in Figure 3, this will not change the general pattern. In addition, while channel forming floods are mainly associated with equal mobility of a large range of sediment particles, the formation of an imbricated fabric involves the clustering of individual clasts only. We use these arguments to justify our preference for using equation 1a (incipient motion of clasts) rather than equation 1b (channel forming floods) (please see lines 488-500).

### **The importance of protrusion effects on the entrainment of large clasts, and the consequences on the Shields variable $\phi$**

This is a major point, because the consequence of protrusion effects is a lowering of the Shields variable  $\phi$  to a value as low as 0.03, with the result that supercritical conditions will not establish. We made a major effort to argue why protrusion effects are likely not to reduce the thresholds and thus the  $\phi$ -values, at least for the mountainous streams we have encountered in the Swiss Alps. We included the following text in our revised manuscript: *Larger bed surface grains, as is the case for most of the imbricated clasts, may exert lower mobility thresholds because of a greater protrusion and a smaller intergranular friction angle, as noted by Buffington and Montgomery (1997) in their review. Related consequences have been explored in experiments (e.g., Buffington et al., 1992) and through field-based studies, which were likewise complemented with experiments in the laboratory (Johnston et al., 1998). These studies resulted in the notion that the entrainment of the largest clasts (e.g., the  $D_{84}$ ) most likely requires lower flow strengths than the shift of median-sized sediment particles. As a consequence, while  $\phi$ -values might be as high as 0.1 for the displacement of the  $D_{50}$  (Buffington et al., 1992), conditions for the incipient dislocation of large clasts could be significantly different. In particular, for clasts that are up to five times larger than the  $D_{50}$  (which corresponds to the ratio between the  $D_{84}$  and the  $D_{50}$  of the Swiss data, Table 1), Buffington et al (1992) and also Johnston et al. (1998) predicted  $\phi$ -values that might be as low as 0.03 or even less. Related  $\phi$ -values, for instance, have indeed been applied for mountainous streams where the supply of sediment from the lateral hillslopes has been large (van der Berg and Schlunegger, 2012). Large sediment fluxes have been considered to result in a poor sorting and a low packing of the material, and thus in low thresholds particularly for the incipient motion of large clast (Lenzi et al., 2006; van der Berg and Schlunegger, 2012). Our calculations predict that an upper flow regime is very unlikely to establish at these conditions ( $\phi$ -value of 0.03).*

*However, we consider it unlikely that the formation of most of the imbrications, as we did encounter in the analyzed Alpine streams and in the stratigraphic record, were associated with thresholds as low as those proposed by e.g., Lenzi et al. (2006) and van der Berg and Schlunegger (2012). We base our inference on the observation that the analyzed gravel bars display an arrangement where large clasts are generally well sorted and densely packed, both on subaerial (during low water stages) and subaquatic bars. This results in a high interlocking degree of sediment particles within the bars we have encountered in the field. In addition, field inspections showed that the base of most of the large clasts, particularly those in subaquatic bars, are embedded and thus buried in finer grained material, and only very few clasts are lying isolated and flat on their a-b-planes. This implies that the fine-grained sediment particles have to be removed before these clasts can be entrained. In this case, hiding effects associated with  $\phi$ -values  $>0.5$  would possibly be appropriate for the prediction of material entrainment of the finer-grained sediments before the larger clasts can be shifted (Buffington and Montgomery, 1997). As a consequence, a dislocation of these clasts and thus a rearrangement of the sedimentary fabric most likely require that large thresholds have to be exceeded, which is mainly accomplished through high-discharge events with large flow strengths. We thus propose that the use of  $\phi$ -values of c. 0.05, which is commonly used for the entrainment of the  $D_{50}$  (Paola and Moring, 1996), is also adequate for the calculation of the hydrological conditions associated with the fabric we have encountered in the field. We do acknowledge, however, that this hypothesis warrants a test with quantitative data, which we have not available. Please note that the low Froude numbers and thus the low  $\phi$ -values of 0.3 inferred for the Thur and the Birse streams might be underestimated,*

*because photos that were taken during high stage flows of these streams display clear evidence for multiple hydraulic jumps over m-long reaches (Spreafico et al., 2001, p. 71 and 77) (Lines 503-546)*

### **Mismatches between experimental results and our inferences**

A major concern of various reviewers addresses the differences in the conclusions between our work and the results derived from experiments. These reproduce imbrications under steady and lower flow regime conditions either through rolling, sliding, or tilting in response to differential winnowing of the fine-grained material. The result is the formation of channel bed armors. Contrariwise, we suggest that imbrications, particularly of coarse-grained cluster bedforms, record high stage and most likely supercritical floods. Our inference critically depends on the assignment of  $\phi$ -values for the mobilization of clasts. While experimental results suggest that  $\phi$ -values as low as 0.03 (and lower) appear as suitable conditions for the shift of clasts in experiments, we suggest that these thresholds are possibly too low to explain the mobilization of the coarse-grained fraction of the material in our streams. We base our inference on the observation that the coarse-grained material in subaquatic and subaerial bars correspond to bedforms of well-clustered and armored arrangements of clasts. Most important, we consider the mismatch in scales as the major difficulty for comparing laboratory experiments with our natural examples. We devoted a full new section to outline our inferences. The following text is a copy of a new section 4.3 entitled *The formation of imbrications in experiments* where we discuss these points: *Interpretations of the possible linkages between hydrological conditions upon material transport and the formation of imbrications are hampered because experiments have not been designed to explicitly explore these relationships. In addition, as noted by Carling et al. (1992), natural systems differ from the conditions in experiments because of the contrasts in scales. Despite these limitations, it was possible to reproduce the formation of clast imbrications in subcritical flumes (Carling et al., 1992), or at least in the absence of any change in flow regime in many experiments. For instance, Qin et al. (2013) quantified the imbrications that resulted from the experiments by Aberle and Nikora (2006) where flows have been stationary. Carling et al. (1992) additionally showed that the shape of a clast has a strong control on the thresholds for incipient motion, the style of motion, and the degree of imbrication. A similar arrangement of clasts was formed in the experiments by Powell et al. (2016) and Bertin and Friedrich (2018), who reproduced imbrications with low Froude numbers between c. 0.55 and 0.9. Powell et al. (2016) additionally showed that the material can be entrained with  $\phi$ -values as low as 0.03, which is consistent with calculations of Froude numbers for some of the streams in Switzerland. Also during experiments, Johansson (1963) reported particle vibration before entrainment either through rolling or sliding. He noted that imbrication was formed at conditions, which corresponded to the lower flow regime during the flume experiments. Finally, based on field observations, Sengupta (1966) reported examples where imbrication was most likely initiated by the development of current crescents around pebbles that were embedded in sand, and that these processes possibly occurred during lower regime flows. Such eddies preferentially develop at the upstream end of pebbles, which then leads to winnowing of the fine grained sand at the upstream edge and the tilting of this particular clast. Additional sliding, pivoting and vibrating of these sediment particles might then result in the final imbrication. If this process occurs multiple times and affects the sand-gravel interface at various sites, then an armored bed with imbricated clasts can establish without the necessity of supercritical flows, changes in flow regimes, as experimental results have shown (Aberle and Nikora, 2006; Haynes and Pender, 2007). They may even form in response to prolonged periods of sub-threshold flows, as summarized by Ockelford and Haynes (2013).*

*However, inspections of photos illustrating the experimental set up reveal that the surface grains are either flat lying on finer-grained sediments before their entrainment (Figure 3 in Powell et al., 2016), occur isolated on the ground (Figure 2.1b in Carling et al., 1992), or have a low degree of interlocking (Figure 3a in Lamb et al., 2017). Interestingly, the experiment by Buffington et al. (1992) followed a different strategy, where a natural bed-*

surface of a stream was peeled off with epoxy. They subsequently used this peel in the laboratory to approximate a natural channel bed surface (see their Figure 4), on top of which they randomly placed grains with a known size distribution. Buffington and co-authors then measured the friction angle of the overlying grains, based on which they calculated the critical boundary shear stress values  $\phi$ . In all experiments, the surface morphology of the sedimentary material is flat and lacks topographic variations, which we found as reach-scale alternations of riffles, transverse bars and pools in the field. The low  $\phi$ -values of 0.03, which appears to be typical of bed surface conditions that develop in laboratory flumes (Ferguson, 2012), as summarized by Powell et al. (2016), could possibly be explained by these limitations. Furthermore, and probably more relevant, the lengths of the experimental reaches are generally less and range between e.g., 4.4 meters (Powell et al., 2016), 15 meters (e.g., Lamb et al., 2017) and even 20 meters (Aberle and Nikora, 2006). We acknowledge that in most experiments the variables have been normalized through a constant Reynolds number. This normalization also includes the experimental  $D_{50}$ -grain sizes, which are very similar to those we have determined for our selected streams (Litty and Schlunegger, 2017). Nevertheless, we find it really hard to upscale some of the results associated with these experiments to our natural cases where standing waves of 1 m, and even between 5 and 8 meters lengths may occur (our Figures 1B, 5B, 6B), which are not reproducible in the experiments. In addition, Powell et al. (2016) observed that the water surface stayed relatively stable during their experiments, and that the flows were steady and uniform without hydraulic jumps. This contrasts to our natural cases where upper and lower flow regimes alternate over short distances even during low-stage flows. Finally, while winnowing of fine grained material, tilting of clasts and subsequent bed armoring might be a valuable mechanism for the explanation of imbrications during low stage flows in experiments, we consider it unlikely that these results can be directly translated to our field observations. We base our inference on two closely related arguments. First, our reported groups of imbricated clasts tend to be arranged as cluster bedforms (e.g., Figures 6D, 7B), which rather form in response to selective deposition of large clasts than selective entrainment of fine-grained material (Figure 6A). Second, observations (Berther, 2012) and calculations (Litty and Schlunegger, 2017) have shown that effective sediment transport in these streams is likely to occur on decadal time scales (and most likely much shorter; van der Berg and Schlunegger, 2012), at least for subaquatic bars. Sediment transport is then likely to occur over a limited reach only. This means that a large fraction of the shifted material per flood has a local source situated in the same river some hundreds of meters farther upstream where bars are also well armored, thus requiring large thresholds for the removal of clasts. In addition, on subaerial bars, waning stages of floods result in the deposition of fine-grained material and not in the winnowing of sand, as our observations have shown. Accordingly, while low  $\phi$ -values and thus a lower flow regime might be appropriate for predicting the entrainment of the sediment particles in experiments, greater thresholds and thus larger  $\phi$ -values are likely to be appropriate for our natural examples for the reasons we have explained in above. (Lines 588-668)

Based on these arguments, we came to the conclusion that clast imbrications are likely to be associated with supercritical flows provided that (i) channel gradients are steeper than  $c. 0.5^{\circ} \pm 0.1^{\circ}$ , and (ii) large clasts are tightly packed, closely arranged as cluster bedforms and partly embedded in finer-grained sediment, yielding in thresholds that are large enough ( $\phi$ -values  $>0.05$ ) to allow supercritical conditions to occur. As mentioned further above, we thus have modified the title and adjusted the abstract accordingly.

## **Specific points raised by reviewer Wickert**

*Reviewer's comment:*

12. What does "presumably" mean here?

*Our response:*

The text has been specified.

*Reviewer's comment:*

19. What kind of "bed roughness values" are these? Please also note units, if needed.

*Our response:*

This has been specified.

*Reviewer's comment:*

43. considered to record

*Our response:*

Corrected.

*Reviewer's comment:*

62. justifications → justification

*Our response:*

Corrected

*Reviewer's comment:*

92. More precisely, the shear stress exerted by the fluid on the bed (shear stress is not an intrinsic property of the fluid)

93. inertial force

*Our response:*

Both have been corrected.

*Reviewer's comment:*

95. You include "x" as a subscript of D in the denominator but not in the numerator. Please be consistent. (Also, i is typically chosen for size classes, if this is the intent of including it, as it seems to be.)

96. gravitational acceleration

*Our response:*

Both have been corrected.

*Reviewer's comment:*

99-101. You are mixing the use of  $\phi$  as the Shields stress (any applied stress, but made clarify here; I think you want the latter definition.

*Our response:*

Yes indeed; this has been corrected.

*Reviewer's comment:*

103-106. I think that you will need a reference for this claim, and it may be good to discuss which grain sizes will be more likely or less likely to be entrained, as this becomes important in heterogeneous mixtures.

*Our response:*

This has been done.

*Reviewer's comment:*

107-108. Lamb et al. (2008) compile the relevant data from that time.

*Our response:*

We have added this reference.

*Reviewer's comment:*

112. 84th percentile; D84 is the size class at that percentile

*Our response:*

This has been specified.

*Reviewer's comments:*

120. Wong and Parker (2006) noted an error in M-P M's original analysis and suggest a value of 0.0495 for critical Shields stress. (In fact, they suggest two values, with the one that I am writing being for maintaining the  $3/2$  relationship with transport.

*Our response:*

We are grateful for this note and have used the updated  $\phi$ -value of  $0.0495 \approx 0.05$  instead.

*Reviewer's comments:*

122. A channel-forming flood must exceed the threshold of motion, and this equation therefore cannot be correct. For many rivers, the Parker (1978) criterion of channel-forming discharge at approximately 1.2 times critical holds. See Phillips and Jerolmack (2016) and Pfeiffer et al. (2017) for a more recent discussion. This and the previous comment must be propagated through the paper.

*Our response:*

We have addressed this point in a separate section. Please see also our general statement of how we have modified the manuscript.

*Reviewer's comments:*

Furthermore, the MPM relationship that you invoke here is designed for only one size class of gravel that comprises the river. This may be appropriate in some cases for the but does not include the extra boost of mobility given to large grains as a result of protruding from a finer-grained bed. This "hiding factor" is important. It will reduce the effective Shields coefficient ( $\phi$ ), and I expect that not including it will cause your Froude number estimates to be anomalously high.

*Our response:*

We have addressed the issue about hiding and protrusion effects in a separate chapter, as we agree that this has major implications and warrants a careful discussion. Please see our response to the general concerns further above.

*Reviewer's comments:*

Finally, you are missing a  $g$  in this equation. I have checked and you do not seem to propagate this error, so it is probably just a local typo.

126-129. Your reason for this relationship working is about the hydraulic radius, but the other important piece is the steady, uniform flow assumption.

*Our response:*

We have addressed both points in the revised manuscript.

*Reviewer' comments:*

134. 1 "s" in Weisbach

153-155. Manning's  $n$  is a function of grain size; see Gary Parker's work (Parker, 1991) or his e-book. This is also cited (perhaps more conveniently) by Wickert and Schildgen (2018, Eq. 13); you can rearrange this equation to solve for Manning's  $n$ .

178-179. Yes! At incipient motion. I suggest that you use this wording instead of "channel-forming" unless/until you are discussing floods that move significant sediment and reshape the channel.

212. calculation of (instead of "to calculate")

213-214. Do you mean that backwater effects become important?

224-226. Is this a qualitative description of the hiding factor? If so, it would be nice to see estimates better quantified, as the Froude number of the depositional conditions is key to your conclusions

230. It could be good to note that your “roughness” is Darcy-Weisbach friction factor, to be unambiguous.

*Our response:*

We have addressed all points addressed above either through specifications in the text, or through editorial improvements and typo corrections.

*Reviewer’s comment:*

238-241. This may be true, but I am calling this into question on the basis of your using the D84

*Our response:*

This addresses the issue about hiding and protrusion effects, which we have fully discussed in a separate chapter. Please see our answer above.

*Reviewer’s comment:*

242-250. See Lamb (2008) and update this paragraph; I do not think the Shields parameter increase will be as extreme as the Mueller study alone shows.

*Our response:*

Yes indeed. We have adjusted the text accordingly.

*Reviewer’s comments:*

263. Artificial river banks can fundamentally alter the flow hydraulics and the self-regulation of channel width. This artificial narrowing can increase flow velocities and alter the Froude number. Do you know that your knowledge of the hydrograph, the bed shear stress, and the age of the imbrications are all consistent with being from either before or after the modifications were made?

*Our response:*

The values we used and related time scales are all consistent with the chronology of anthropogenic corrections. We have made this point in the revised manuscript.

*Reviewer’s comments:*

320-321. I do not see how a floodplain would confine a gravel-bed river, especially on an aggrading alluvial fan. Could you please explain or change this statement?

349. A general comment on the data section: your focus in the writing is more on the non-imbricated sediments in the geological record and the imbricated sediments in the modern rivers. I think it is important to make clear to the readers that you have both conditions from both environments at the very start.

*Our response:*

We have clarified the first question and taken into consideration the second point.

*Reviewer’ comments:*

<I have stopped making English usage corrections at this point. Several more minor errors follow, but the English is overall quite good.>

432-434. These are the forces driving particle motion, but weight also operates on the particle.

439. Could you use the long axes of the particle in this equation as the lever arm? You have measured them, it appears.

467. Are flow velocities really higher on steeper slopes? Or do roughness and shallower overall flow decrease the velocity proportionately?

471. My reading of the Lamb et al. (2008) study was that it included a significant data-driven component, which has a large compilation; my impression is that you are not taking

into account this compilation and instead prefer the field measurements from Mueller (2005). This choice needs justification.

*Our response:*

We are grateful for the acknowledgement of our usage of the English. We addressed all additional points in the sense that specifications have been added in the text.

## **Specific points raised by reviewer R. Hodges**

*Reviewer's comment:*

Having read the previous two reviews, I agree with the points that they raise. I've also looked at the authors' responses. However, I'm still unconvinced by the argument that imbricated fabrics only form under super-critical flows, and less convinced that strong imbrication will only occur at the specific location of the transition between sub- and super-critical regimes. I agree with Carling that it is not clear from the paper whether you are claiming that imbrication occurs when  $Fr > 1$ , or only at the locations where flow is transitioning at a hydraulic jump. If it is the latter case, then how do you reconcile the widespread occurrence of imbrication across bars with the limited spatial extent of hydraulic jumps? Could you predict the spatial occurrence of hydraulic jumps and see whether that matched the spatial occurrence of imbrication?

*Our response:*

We suggest that imbrication occurs when  $Fr > 1$ . Clusters of imbricated clasts might then result in hydraulic jumps, as is particularly observed during low water stages. We have clarified this issue in the revised version of our manuscript.

*Reviewer's comment:*

There are some flume studies that are relevant to your work which demonstrate imbricated fabrics forming in subcritical flows. Burtin and Friedrich (2018) demonstrate imbrication in flows with  $Fr = 0.54$  and  $0.55$  (calculated from their Table 2). Powell et al (2016) demonstrate imbrication in flows with  $Fr \approx 0.60$  to  $\approx 0.94$ , with the amount of imbrication not varying with  $Fr$ . ( $Fr$  is calculated using their stated slopes, depth and roughness ratio, and your equations 6 and 8). Are these data consistent with your argument?

*Our response:*

We have discussed this issue in a separate section in the discussion (new section labelled "The formation of imbrications in experiments"). Please see our explanations above.

*Reviewer's comment:*

I think that Figure 3 could be clearer, and is potentially misleading. Panels A/B and C/D show different things;  $Fr$  values in A/B and imbrication in C/D. By using the same colour scheme across all panels you are equating imbrication with  $Fr > 1$ , but it's hard to tell whether the data support this. I can see that as slope increases,  $Fr$  is likely to be  $> 1$  and more imbrication is observed. The pattern with bed roughness is less clear. In B  $Fr > 1$  is most likely at intermediate roughness, however the imbrication all occurs at high roughness. The sites with no imbrication occur at the sort of roughness values that correspond to the highest  $Fr$  values; therefore the two patterns don't look similar to me. Why not calculate the  $Fr$  values for entrainment of D84 in the field and rock deposits, and see whether you get a consistent pattern between the  $Fr$  value and whether imbrication is observed?



*Our response:*

We have separated the two figures and changed the colours in order to avoid this confusion. We have not specifically calculated the F-values for the field data mainly because this will heavily depend on channel slope and the bed roughness values, and particularly on the  $\phi$ -values. However, we modified the discussion to make the linkage between field-based observations and modelling results more transparent and clearer. Please see lines 640-692 of our revised manuscript.

*Reviewer's comment:*

I would have liked to see some attempt to quantify the amount of imbrication that is observed in the field and rocks. In your response to Carling you refer to shallow and strongly dipping grains, and suggest that the former might form under sub-critical flows. If this is the case, then your argument is not as simple as imbrication equals super-critical flows. You would need a more robust method to quantify the amount of imbrication, and a dataset to determine the relationship between imbrication amount and flow regime.

*Our response:*

Unfortunately, we don't have quantitative data to properly constrain these observations. We therefore frame our hypothesis around other arguments. We provide evidence from the field, documenting that sites with imbrications are also the reaches where we observed supercritical flows during high stages. Please see lines 665-677 of the revised manuscript.

*Reviewer's comment:*

As with Carling, I'm also unconvinced by the argument that grain rolling is necessary for imbrication to occur. I would have thought it possible for a grain to be entrained by sliding, and to slide or flip into an imbricated position on deposition. There is also evidence that beds can undergo some restructuring at sub-critical flows, which has potential to include imbrication.

*Our response:*

We agree and we have removed this section.

*Reviewer's comment:*

19: I'm not convinced that this description of a threshold is consistent with Fig 3 and later parts of the paper, in which you describe Fr values decreasing again at high slopes and roughness values.

*Our response:*

Our results reveal that imbrications possibly record supercritical flows provided that (i)  $\phi$ -values are larger than c. 0.05, which might be appropriate for streams in the Swiss Alps; (ii) average stream gradients exceed c.  $0.5 \pm 0.1^\circ$ ; and that (iii) relative bed roughness values, i.e. the ratio between the water depth  $d$  and the  $D_{84}$ , are larger than  $\sim 0.06 \pm 0.01$ . We have clarified these points in the revised manuscript.

*Reviewer's comment:*

119: I agree with Wickert that you need to consider hiding effects. The stated Shield's criterion values of 0.03 to 0.06 normally refer to D50, and in the case of hiding effects (i.e. in most gravel beds) then the Shields value of D84 would be less than for D50. In your response you argue that imbricated grains would be harder to move, and there- fore a

higher value is appropriate; however, if you are considering how grains become imbricated from a non-imbricated bed, then you don't need to make this adjustment. It's important to address this issue, because the dimensionless critical shear stress that you use affects whether you reach super-critical flows in Fig 3. If a value less than 0.047 is most appropriate, then it doesn't support your argument about the importance of super-critical flows.

*Our response:*

We agree that hiding and protrusion effects are relevant, and that these have a measurable influence on the  $\phi$ -values and thus on the outcome of our calculations. We discussed the related effects in a separate chapter. We actually find that because most of the largest clasts are either embedded in finer-grained particles, or form well-sorted and densely packed clusters, the finer grained material has to be removed before the largest grains can be entrained. This actually calls for the consideration of hiding effects with larger thresholds. We have discussed this point in full detail in lines 499-543.

*Reviewer's comment:*

122: Don't include 0.047 in eq. 3; use  $\phi$  instead as this is consistent with what you show later on when this equation gets combined with others in equations 9 and 10.

*Our response:*

This has been done.

*Reviewer's comment:*

225: You do refer here to the idea of sorting, and therefore hiding, effects affecting the value of  $\phi$ , but this would be better explained earlier on when you are considering the appropriate value of  $\phi$ .

*Our response:*

This has been done.

*Reviewer's comment:*

305: I assume that you are looking at exposures that are parallel to the flow direction, but you don't state whether this is the case. The amount of imbrication that you observe is likely to be affected by the direction of the exposure with respect to the flow direction.

*Our response:*

We are looking parallel to the flow direction. We have clarified this point.

*Reviewer's comments*

350: It might be useful to have a summary of which exposures shows imbrication and which didn't.

*Our response:*

The sites/sections which bedrock with or without imbrications are shown on e.g., Figure 2 in Garefalakis and Schlunegger (2018) and in Schlunegger and Norton (2015). We refer to these articles where sites of the sections including the corresponding units are shown and illustrated.

*Reviewer's comments*

373: It's not obvious to me how eq. 1 explains the decrease in Fr at high slopes and high roughness. This could be more clearly explained. See Lamb et al. (2017) for analysis of the relationships between flow resistance, flow depth and slope.

*Our response:*

We acknowledge that we have not correctly interpreted these trends. Indeed, the tendency towards lower Froude numbers for a channel gradient  $>1^\circ$  ( $\phi >0.05$ ) and a bed roughness  $>0.3$  ( $\phi >0.05$ ) is somewhat unexpected. We explain these trends through the non-linear relationships between slope, water depth, the energy loss within the roughness-layer, and the velocity at the flow's surface.

*Reviewer's comments*

423: Changes with slope depend on whether flow depth and hence relative roughness also changes.

*Our response:*

Indeed. However, we have removed this entire section, because the following statements about rolling/sliding have not convinced P. Carling either.

*Reviewer's comment:*

449: I don't follow the argument here. I think that you're arguing that because of the pivot angle, then  $\phi$  should be greater than the typical 0.03 to 0.06? You don't need imbrication to get pivot angles greater than 5 to 10° though. Most gravel grains have higher pivot angles; see Kirchner et al. (1990), Buffington et al. (1992) and Johnston et al. (1998) among others.

*Our response:*

We have removed this entire section as none of the reviewers has been fully convinced by this.

*Reviewer's comment:*

583: Where or how are the data available?

*Our response:*

Actually, the grain size data and other material (Table 1) we have used have already been published, and all new material we have used are presented this article. This means that this particular statement becomes obsolete, so we have removed it.

## **Specific points raised by reviewer S. McLelland**

*Reviewer's comment:*

Comments by line (I've avoided repeating comments already made by others): 50: The diagram suggests that hydraulic jumps occur at a grain-scale (as shown in Figure 1 and later in Fig 5)? Is this a representative of realistic situations?

*Our response:*

Yes, it is. We have mentioned this in the revised version.

*Reviewer's comment:*

169: It's not clear why sediment structures are associated with 'channel forming floods'. As

experiments have shown, bed structuring can take place as mobile or static armours develop which may be just high flow events rather than channel forming events.

*Our response:*

This relates to the same comment by A. Wickert. We have corrected the text accordingly.

*Reviewer's comment:*

288: Are these groups of imbricated clasts cluster bedforms or are they just embedded in the bed structure? It would be useful to distinguish whether or not your structures are clusters both in terms of the moderns streams and stratigraphic record.

*Our response:*

These are indeed cluster bedforms. We have specified the text accordingly.

*Reviewer's comment:*

355: You use  $D/d$  in text, but  $D84/d$  in equations.

373: Equation 1 does directly related to flow depth ( $d$ ) or  $D84$

*Our response:*

Both address the same point. We have corrected the text accordingly.

Thank you very much for handling our work.

Sincerely

The authors

## References:

- Aberle, J., and Nikora, V., Statistical properties of armored gravel bed surfaces, *Water Resour. Res.*, 42, W11414, 2006.
- Bertin, S., and Friedrich, H., Effect of surface texture and structure on the development of stable fluvial armors, *Geomorphology*, 306, 64-79, 2018.
- Berther, R., Geomorphometrische Untersuchungen entlang der Entle, Ms. Thesis, Univ. Bern, Bern, Switzerland, 94 p., 2012.
- Buffington, J., Dietrich, W.E., and Kirchner, J.W., Friction angle measurements on a naturally formed gravel streambed: Implications for critical boundary shear stress, *Water Res. Res.*, 28, 411-425, 1992.
- Buffington, J.M., and Montgomery, D. R., A systematic analysis of eight decades of incipient motion studies, with special reference to gravel-bedded rivers, *Water Resour. Res.*, 33, 1993-2029, 1997.
- Carling, P.A., Kelsey, A., and Glaister, M.S., Effect of bed roughness, particle shape and orientation on initial motion criteria, in: *Dynamics of gravel-bed rivers*, edited by: Billi, P., Hey, R.D., Throne, C.R., and Tacconi, P., 23-39. John Wiley and Sons, Ltd., Chichester, 1992.
- Ferguson, R., River channel slope, flow resistance, and gravel entrainment thresholds, *Water Resour. Res.*, 48, W05517, doi:10.1029/2011WR010850, 2012.
- Haynes, H., and Pender, G., Stress history effects on graded bed stability, *J. Hydraul. Eng.*, 33, 343-349, 2007.
- Johansson, C.E., Orientation of pebbles in running water: a laboratory study, *Geogr. Ann.*, 45, 85-112, 1963.
- Johnston, C.E., Andrews, E.D., and Pitlick, J., In situ determination of particle friction angles of fluvial gravels, *Water Resour. Res.*, 34, 2017-2030, 1998.
- Lamb, M.P., Brun, F., and Fuller, B.M., Hydrodynamics of steep streams with planar coarse-grained beds: Turbulence, flow resistance, and implications for sediment transport, *Water Resour. Res.*, 53, 2240-2263, 2017.
- Lenzi, M.A., Mao, I., and Comiti, F., When does bedload transport begin in steep boulder-bed streams?, *Hydrol. Proc.*, 20, 3517-3533, 2006.
- Litty, C., and Schlunegger, F., Controls on pebbles' size and shapes in streams of the Swiss Alps, *J. Geol.*, 123, 405-427, 2017.
- Ockelford, A.-M., and Haynes, H., The impact of stress history on bed structure, *Earth Surf. Process. Landf.*, 38, 717-727, 2013.

- Paola, C., and Moring, D., Palaeohydraulics revisited: palaeoslope estimation in coarse-grained braided rivers. *Basin Res.*, 8, 243-254, 1996.
- Parker, G., Self-formed straight rivers with equilibrium banks and mobile bed. Part 2. The gravel river, *J. Fluid Mech.*, 89, 127-146, 1978. doi:10.1017/S002112078002505.
- Pfeiffer, A.M., Finnegan, N.J., and Willenbring, J.K., Sediment supply controls equilibrium channel geometry in gravel rivers, *Proc. Natl. Acad. Sci. U.S.A.*, 114, 3346-3351, 2017.
- Philips, C.B., and Jerolmack, D.J., Self-organization of river channels as a critical filter on climate signals, *Science*, 352, 649-697, 2016.
- Powell, M.D., Ockelford, A., Rice, S.P., Hillier, J.K., Nguyen, T., Reid, I., Tate, N.J., and Ackerley, D., Structural properties of mobile armors formed at different flow strengths in gravel-bed rivers. *J. Geophys. Res. – Earth Surface*; 121, 1494-1515, 2016.
- Qin, J., Zhong, D., Wang, G., and Ng, S.L., Influence of particle shape on surface roughness: Dissimilar morphological structures formed by man-made and natural gravels, *Geomorphology*, 190, 16-26, 2013.
- Sengupta, S., Studies on orientation and imbrication of pebbles with respect to cross-stratification, *J. Sed. Petrol.*, 36, 227-237, 1966.
- Van der Berg, F., and Schlunegger, F., Alluvial cover dynamics in response to floods of various magnitudes: The effect of the release of glaciogenic material in a Swiss Alpine catchment, *Geomorphology*, 141, 121-133, 2012.

# Clast imbrications in coarse-grained mountainous streams and stratigraphic archives possibly suggest deposition under upper flow regime conditions

Fritz Schlunegger, Philippos Garefalakis  
Institute of Geological Sciences  
University of Bern, Switzerland  
fritz.schlunegger@geo.unibe.ch  
philippos.garefalakis@students.unibe.ch

## Abstract

Clast imbrications are one of the most conspicuous sedimentary structures in coarse-grained clastic deposits, of modern rivers but also in the stratigraphic record. In this paper, we test whether the formation of such a fabric could be related to the occurrence of upper flow regime conditions in streams. To this extent, we calculated the Froude number at the incipient motion of coarse-grained bedload for various values of relative bed roughness and stream gradient, as these are the first order variables that can particularly be extracted from stratigraphic records. We found that a steeper energy gradient, or slope, and a larger bed roughness tend to favor the occurrence of supercritical flows. We also found that at the incipient motion of grains, the ratio  $\phi$  between the critical shear stress for the entrainment of a sediment particle and its inertial force critically controls whether flows tend to be super- or subcritical during sediment entrainment. We then mapped the occurrence of clast imbrications in Swiss streams and compared these data with the outcomes of the hydrologic calculations. The results reveal that imbrications possibly record supercritical flows provided that (i)  $\phi$ -values are larger than c. 0.05, which might be appropriate for streams in the Swiss Alps; (ii) average stream gradients exceed c.  $0.5 \pm 0.1^\circ$ ; and that (iii) relative bed roughness values, i.e. the ratio between the water depth  $d$  and the  $D_{3,4}$ , are larger than  $-0.06 \pm 0.01$ . While we cannot rule out that imbrication may be formed during subcritical flows with  $\phi$ -values as low as 0.03, as a large number of flume experiments reveal, our results from Alpine streams suggest that clast imbrications are likely recorders of upper flow regime conditions, provided that the clasts form well-sorted and densely packed clusters. We consider that these differences may be rooted in a misfit between the observational and experimental scales.

## 1 Introduction

Conglomerates, representing the coarse-grained spectrum of clastic sediments, bear key information about the provenance of the material (Matter, 1964), the environment in which these sediments were deposited (Rust, 1978; Middleton and Trujillo, 1984),

- geo Uni Bern 30.7.2018 22:11  
**Style Definition:** Comment Text
- geo Uni Bern 30.7.2018 22:11  
**Deleted:** sediments
- geo Uni Bern 30.7.2018 22:11  
**Deleted:** changes from
- geo Uni Bern 30.7.2018 22:11  
**Deleted:** to lower
- geo Uni Bern 30.7.2018 22:11  
**Deleted:** presumably
- geo Uni Bern 30.7.2018 22:11  
**Deleted:** .
- geo Uni Bern 30.7.2018 22:11  
**Deleted:** is
- geo Uni Bern 30.7.2018 22:11  
**Deleted:** changes from lower to
- geo Uni Bern 30.7.2018 22:11  
**Deleted:** calculate
- geo Uni Bern 30.7.2018 22:11  
**Deleted:** . We then compare the results with data from modern streams and
- geo Uni Bern 30.7.2018 22:11  
**Deleted:** The
- geo Uni Bern 30.7.2018 22:11  
**Deleted:** show that upper flow regime conditions most likely establish where
- geo Uni Bern 30.7.2018 22:11  
**Deleted:** °, and where relative bed roughness values are larger than  $-0.06 \pm 0.01$ . Similarly, data from modern streams reveal that imbricated clasts are found where channels are steeper than c.  $0.5 \pm 0.2^\circ$ , and where
- geo Uni Bern 30.7.2018 22:11  
**Deleted:** exceed  $-0.07$ . Likewise, imbricated conglomerates are encountered in late Oligocene foreland basin sequences where paleo-slopes were greater than  $0.4^\circ$ . We use these relationships to propose that clast imbrications occur where channel gradients exceed a threshold, which appears large enough for upper flow regime conditions to establish. We finally relate the formation of an imbricated arrangement of clasts to a mechanism where material transport occurs through rolling, or pivoting. This process requires a large shear force and thus
- geo Uni Bern 30.7.2018 22:11  
**Deleted:** flow velocity upon transport, which is likely to be associated with ... (1)
- geo Uni Bern 30.7.2018 22:11  
**Deleted:** thus
- geo Uni Bern 30.7.2018 22:11  
**Deleted:** suitable
- geo Uni Bern 30.7.2018 22:11  
**Deleted:** upon sediment transport
- geo Uni Bern 30.7.2018 22:11  
**Formatted:** Font color: Auto

82 and the hydro-climatic conditions upon transport and deposition of the sediments  
83 (Duller et al., 2012; D'Arcy et al., 2017). Conglomerates display the entire range of  
84 possible sedimentary structures including a massive-bedded fabric, cross-beds and  
85 horizontal stratifications. However, the most striking features are clast imbrications  
86 (Figure 1A), which refer to a depositional fabric where sediment particles of similar  
87 sizes overlap each other, similar to a run of toppled dominoes (e.g., Pettijohn, 1957;  
88 Yagishita, 1997; Rust, 1984; Potsma and Roep, 1985; Todd, 1996). Imbrications may  
89 lead to armor development and the interlocking of clasts. As a consequence the search  
90 for possible controls on the formation of this fabric has received major attention in the  
91 literature (e.g., Bray and Church, 1980; Carling, 1981; Aberle and Nikora, 2006).

92 In the past decades, the occurrence of clast imbrications in streams has been  
93 considered to record high stage flows (Rust, 1978; Miall, 1978; Sinclair and Jaffey,  
94 2001). The related conditions could possibly correspond to the upper flow regime,  
95 where the flow velocity of a stream  $v$  exceeds the wave's celerity  $c$  (Allen, 1997), i.e. the  
96 speed of a wave on the water surface. The ratio  $v/c$  between these velocities has been  
97 referred to as the Froude number  $F$  where in theory  $F > 1$  denotes upper flow or  
98 supercritical conditions, while  $F < 1$  is characteristic for the lower flow regime or alternatively  
99 subcritical conditions (Engelund and Hansen, 1967). A hydraulic jump, which is  
100 characterized by a distinct increase in flow surface elevation and a decrease in flow  
101 velocity, then marks the downstream transition from a super- to a subcritical flow (Figure  
102 1A). These hydrological conditions are particularly mirrored by the surface texture in  
103 relation to water depth. Surface waves that form under subcritical conditions have  
104 wavelengths that are smaller than the water depths (Figure 1B). The surface waves tend to  
105 migrate and fade out in the upstream direction with respect to the flow. Contrariwise, the  
106 wavelengths of standing waves, which represent one possible characteristic feature of  
107 supercritical conditions ( $F \approx 1$ ), are significantly larger than the corresponding water depths,  
108 and the surface waves are stationary. Hydraulic jumps are manifested themselves by a  
109 sudden deceleration of the flow velocity and by an overturning of the flow surface (Figure  
110 1).

111 Significant sediment accumulation may occur underneath the hydraulic jump upon  
112 deceleration of the flow's velocity (Slootman et al., 2018). Contrariwise, a downstream  
113 change from a lower to an upper flow regime occurs gradually and has no distinct surface  
114 expression, neither in terms of flow depth nor flow surface texture. While these  
115 mechanisms have been well explored and frequently reported both from modern  
116 environments (e.g., Figure 1) and fine grained stratigraphic records (Alexander et al.,  
117 2001; Schlunegger et al., 2017; Slootman et al., 2018) and illustrated on photos from the  
118 field (Spreafacio et al., 2001), less evidence for an upper flow regime has been  
119 documented from the coarse grained fraction of clastic sediments such as conglomerates.  
120 This even led Grant (1997) to note that upper flow regime conditions in fluvial channels are

geo Uni Bern 30.7.2018 22:11

Deleted: 1

geo Uni Bern 30.7.2018 22:11

Deleted: clasts

geo Uni Bern 30.7.2018 22:11

Deleted: as primary recorders of

geo Uni Bern 30.7.2018 22:11

Deleted: most likely

geo Uni Bern 30.7.2018 22:11

Deleted: 1).

126 rare, and that the use of the Froude number for constraining flood and **palaeo**-flood  
 127 measurements lacks **justification** from sedimentary records. In the same sense, Jarrett  
 128 (1984) and Trieste (1992, 1994) considered that reports of inferred supercritical flows  
 129 might be biased by underestimations of the bed roughness in mountainous streams.  
 130 **Nevertheless, the surface texture of the flow illustrated in Figure 1A is characteristic for**  
 131 **many mountainous streams (Spreafico et al., 2001), where hydraulic jumps are observed**  
 132 **on the stoss side of large imbricated clasts. In addition,** because the entrainment of large  
 133 clasts such as cobbles and boulders does involve large shear stresses and thus high  
 134 discharge flows (Rust, 1978; Miall, 1978; Sinclair and Jaffey, 2001), it is possible that the  
 135 transport and deposition of these particles, and particularly the formation of an imbricated  
 136 fabric, **may occur during supercritical flows.** Here, we **explore the validity of this hypothesis**  
 137 **for modern coarse-grained streams and stratigraphic records, and we calculate the related**  
 138 **hydrological conditions.** Similar to Grant (1997), we **determine** the Froude number at  
 139 conditions of incipient motion of coarse-grained bedload for various bed roughness and  
 140 stream gradient values. We **then** compare the results with data from modern streams **in**  
 141 **the Swiss Alps,** stratigraphic records and **published results of laboratory experiments.**

geo Uni Bern 30.7.2018 22:11  
 Deleted: paleo

geo Uni Bern 30.7.2018 22:11  
 Deleted: justifications

geo Uni Bern 30.7.2018 22:11  
 Deleted: Nevertheless

geo Uni Bern 30.7.2018 22:11  
 Deleted: is indeed related to changes in flow regimes (Figure 1).

geo Uni Bern 30.7.2018 22:11  
 Deleted: test

geo Uni Bern 30.7.2018 22:11  
 Deleted: fluvial sediments

geo Uni Bern 30.7.2018 22:11  
 Deleted: .

geo Uni Bern 30.7.2018 22:11  
 Deleted: calculate

geo Uni Bern 30.7.2018 22:11  
 Deleted: and

geo Uni Bern 30.7.2018 22:11  
 Deleted: suggest that imbricated clasts are likely to provide evidence for supercritical flows, or at least for changes from upper to lower flow regimes over short distances (Figure 1).

geo Uni Bern 30.7.2018 22:11  
 Deleted: .

geo Uni Bern 30.7.2018 22:11  
 Formatted: Font:Not Italic

geo Uni Bern 30.7.2018 22:11  
 Deleted: paleo

geo Uni Bern 30.7.2018 22:11  
 Deleted: sedimentological

geo Uni Bern 30.7.2018 22:11  
 Deleted: a

geo Uni Bern 30.7.2018 22:11  
 Deleted: critical shear stress

geo Uni Bern 30.7.2018 22:11  
 Deleted: fluid's

geo Uni Bern 30.7.2018 22:11  
 Deleted:  $\tau_{cDx}$

geo Uni Bern 30.7.2018 22:11  
 Deleted: inertia

geo Uni Bern 30.7.2018 22:11  
 Deleted:  $\phi = \frac{\tau_{cDx}}{(\rho_s - \rho)gD_x}$   
 Deleted: ..... (1).

## 2 Methods

### 2.1 Expressions relating flow regime to channel gradient and bed roughness

Channel depth and grain size are the simplest and most straightforward variables that can be extracted from stratigraphic records (Duller et al., 2012). It has been shown that quantitative information about these variables can be used as basis to calculate **palaeo**-slope and roughness values of streams for the geologic past (Paola and Mohring, 1996; Duller et al., 2012; Schlunegger and Norton, 2015; Garefalakis and Schlunegger, 2018). We therefore decided to focus on the simplest expressions relating channel depth and grain size to flow strength and sediment transport, such as that the resulting formulas can also be applied to **geological** records. We are aware that this will be associated with large generalizations and simplifications, which will not consider the entire range of complexities that are usually associated with the transport of coarse-grained bedload in streams.

### 2.2 Boundary conditions

In the following, we consider the hydrological situation at the incipient motion of coarse-grained bedload. For these conditions, **the** dimensionless **Shields parameter**  $\phi$  can be computed, which is the ratio between the **shear stress exerted by the fluid on the bed**  $\tau_{cDi}$  and the particle's **inertial force at the incipient motion** (Shields, 1936; Paola et al., 1992; Paola and Mohring, 1996; Tucker and Slingerland, 1997):

$$\phi = \frac{\tau_{cDi}}{(\rho_s - \rho)gD_i} \quad (1a).$$



188 Here,  $\tau_{cD_i}$  denotes the critical shear stress, or alternatively the Shields stress, which is  
 189 required to shift a sediment particle with the grain size  $D_i$ . The constants  $\rho_s$  (2700  
 190  $\text{kg/m}^3$ ) and  $\rho$  denote the sediment and water densities, and  $g$  is the gravitational  
 191 acceleration. The relationship expressed in equation (1a) predicts that a sediment  
 192 particle with diameter  $D_i$  will be transported if the ratio between the fluid's shear stress  
 193  $\tau_{cD_i}$  and the particle's inertial force equals the value of  $\phi$ . Assignments of values to  
 194  $\phi$  vary considerably and largely range between c. 0.03 and 0.06, depending on the site-  
 195 specific arrangement, the sorting, and the interlocking of the clasts (Buffington and  
 196 Montgomery, 1997; Church, 1998). This also includes the hiding and protrusion of small  
 197 and large clasts, respectively, which may exert a strong influence on the threshold  
 198 conditions upon clast entrainment (e.g., Egiazaroff, 1965; Parker et al., 1982; Andrews,  
 199 1984; Kirchner et al., 1990). In the same sense, a smooth and flat channel bed surface,  
 200 which may be a well-armored channel floor with well-sorted clasts, is likely to offer a  
 201 greater resistance for the entrainment of a sediment particle than a gravel bar with a poorly  
 202 sorted arrangement of the bed material (Egiazaroff, 1965; Buffington and Montgomery,  
 203 1997).

204 The relationships denoted in equation (1a) differ for the case of channel forming floods. At  
 205 these conditions, channel forming Shield stresses  $\tau_{channel}$  are up to 1.2 times (Parker, 1978)  
 206 above the threshold  $\tau_{cD_i}$  for the initiation of motion. Pfeiffer et al. (2017) additionally  
 207 showed that some rivers have  $\tau_{channel}/\tau_{cD_i}$  ratios that are even higher. The consideration of  
 208 channel forming floods thus requires larger thresholds and thus a modification of equation  
 209 (1a), which then takes the following form:

$$210 \phi' \geq \frac{\tau_{channel}}{(\rho_s - \rho)gD_i} \approx 1.2 \frac{\tau_{cD_i}}{(\rho_s - \rho)gD_i} = 1.2\phi \quad (1b).$$

211 Equation (1a) can then be transformed to an expression, which quantifies the critical shear  
 212 stress for the entrainment of a sediment particle with a distinct grain size  $D_i$ :

$$213 \tau_{cD_i} = \phi(\rho_s - \rho)gD_i \quad (2).$$

214 Among the various grain sizes, the  $D_{84}$  grain size has been considered as more  
 215 suitable for the characterization of the gravel bar structure than the  $D_{50}$  (Howard, 1980;  
 216 Hey and Thorne, 1986; Grant et al., 1990). In addition, the  $D_{84}$  has also been  
 217 considered as a valuable parameter for the quantification of the relative bed  
 218 roughness, which is defined as the ratio between grain size and water depth (e.g.,  
 219 Wiberg and Smith, 1991). If this inference is valid, then a major alteration of channel-  
 220 bar arrangements requires a flow strength that is large enough to entrain the grain size  
 221 represented by the 84<sup>th</sup> percentile.

222 Based on the results of flume experiments (Meyer-Peter and Müller, 1948) and  
 223 observations in the field (Andrews, 1984), a Shields variable of  $\phi=0.047$  has

geo Uni Bern 30.7.2018 22:11  
 Deleted: g is the gravity accelerat... [2]

geo Uni Bern 30.7.2018 22:11  
 Formatted: Font:Italic

geo Uni Bern 30.7.2018 22:11  
 Deleted:  $D_x$

geo Uni Bern 30.7.2018 22:11  
 Formatted

geo Uni Bern 30.7.2018 22:11  
 Deleted: grain size of interest

geo Uni Bern 30.7.2018 22:11  
 Formatted: Expanded by 0.2 pt

geo Uni Bern 30.7.2018 22:11  
 Deleted: 1...a) predicts that a sedi... [4]

geo Uni Bern 30.7.2018 22:11  
 Deleted: well-sorted gravel bars... [5]

geo Uni Bern 30.7.2018 22:11  
 Deleted:  $D_x$

geo Uni Bern 30.7.2018 22:11  
 Deleted:  $\tau_{cD_x} = \phi(\rho_s - \rho)gD_x$

geo Uni Bern 30.7.2018 22:11  
 Formatted: Font:Times

geo Uni Bern 30.7.2018 22:11  
 Deleted: percentile...rain size has... [6]

geo Uni Bern 30.7.2018 22:11  
 Deleted:  $\tau_{cD_{84}} = 0.047 * (\rho_s - \rho)D_{84}$   
 .....(3) -

271 conventionally been employed in a large number of studies (e.g., Paola and Moring,  
 272 1996) particularly if the  $D_{50}$  is considered. Note that a re-analysis (Wong and Parker,  
 273 2006) of the Meyer-Peter and Müller equation (1948) returned values of  
 274  $\phi=0.0495\approx 0.05$ , which we thus applied in this paper. However, experiments also  
 275 showed that material transport can occur at much lower thresholds where  $\phi$ -values are  
 276 as low as 0.03 (Ferguson, 2012; Powell et al., 2016). A  $\phi$ -value of 0.03 might  
 277 particularly be an appropriate threshold for the entrainment of the  $D_{84}$ , because of  
 278 possible protrusion effects (e.g., Kirchner et al., 1990). Finally, Mueller et al. (2005) and  
 279 Lamb et al. (2008) proposed that  $\phi$  depends on channel gradients, where  $\phi$  (for the  $D_{50}$   
 280 grain size) might exceed 0.1 for channels that are steeper than  $1.1^\circ$ . It appears that the  
 281 thresholds for the entrainment of sediment strongly vary according to site and  
 282 experiment specific conditions. We therefore employed the entire range of  $\phi$ -values  
 283 from 0.03 to 1.1 to comply with these complexities, which also includes channel  
 284 forming floods (Parker, 1978).

### 286 2.3 Hydrology, bed shear stresses and incipient motion of clasts

287 Bed shear stress is calculated using the approximation for an uniform flow down an  
 288 inclined plane (e.g. Tucker & Slingerland, 1997), where:

289 
$$\tau = g\rho Sd \tag{3}$$

290 Here,  $S$  denotes the channel gradient, and  $d$  is the water depth. This relationship has been  
 291 considered as adequate for streams with a steady, uniform flow, and where channel  
 292 widths are more than 20 times larger than water depths, which is commonly the case for  
 293 most rivers (Tucker and Slingerland, 1997).

294 Alternatively, bed shear stresses can also be computed as a function of the kinetic energy  
 295 (Ferguson, 2007), where:

296 
$$\tau = \frac{f}{8} \rho v^2 \tag{4}$$

297 In this relationship,  $v$  is the flow velocity. The variable  $f$ , referred to as the Darcy-Weisbach  
 298 friction factor (e.g., Papaevangelou et al., 2010), denotes the energy loss due to friction  
 299 within the roughness layer at the bottom of the flow. It also considers skin friction effects  
 300 within the flow column (Ferguson, 2007). These relationships illustrate that assignments of  
 301 values to  $f$  are complicated and vary considerably. Ferguson (2007) reduced these  
 302 complexities to a single expression (equation 5), where he considered roughness-layer  
 303 (Krogstad and Antonia, 1999) and skin friction effects on the velocity of a water column at  
 304 its surface. In the Ferguson (2007) relationship,  $f$  depends on water depths  $d$  relative to the  
 305 grain size  $D_{84}$  and thus on the relative bed roughness:

geo Uni Bern 30.7.2018 22:11  
 Deleted: 4

geo Uni Bern 30.7.2018 22:11  
 Deleted: 5

geo Uni Bern 30.7.2018 22:11  
 Deleted: Weissbach

geo Uni Bern 30.7.2018 22:11  
 Deleted: Within the flow boundary layer, energy loss appears to be lower for channel floors with well-sorted gravel bars than poorly sorted ones. The same is the case for the characteristic grain size  $D_x$ , where larger grains exert a greater frictional resistance on the flow than smaller ones.

geo Uni Bern 30.7.2018 22:11  
 Deleted: 6

318 
$$\frac{f}{8} = \frac{\left(\frac{D_{84}}{d}\right)^2}{a_2^2} + \frac{\left(\frac{D_{84}}{d}\right)^{1/3}}{a_1^2} \quad (5).$$

319 Here,  $a_1$  and  $a_2$  are constants that vary between 7–8 and 1–4, respectively (Ferguson,  
 320 2007). A calibration of equation 5 by Ferguson (2007), where the  $D_{84}$  was employed as the  
 321 threshold grain size, returned values of 7.5 and 2.36 for  $a_1$  and  $a_2$ , respectively, which we  
 322 adapt in this paper. We additionally considered possible consequences of energy loss  
 323 through assignments of different values to the Shields (1936) variable (see explanation of  
 324 equation 1a above). We are aware that we could also employ the Manning's number  $n$   
 325 for the characterization of the channel's fabric (Whipple, 2004) and the relative bed  
 326 roughness (Jarrett, 1984). Related expressions deviated by Jarrett (1984) predict that  
 327 the Manning's number  $n$  hinges on the channel gradient and water depth only and does  
 328 not consider a dependency on the bed structure. We thus prefer to use Ferguson's  
 329 (2007) approach (eq. 5), which explicitly includes the relative bed roughness,  
 330 consistent with the most recent work by Wickert and Schildgen (2018, see their  
 331 equation 13).

332 As outlined in the introduction, the Froude number  $F$  can be approximated through the  
 333 ratio between the flow velocity  $v$  and the celerity of a surface wave  $c$ . For shallow water  
 334 conditions, which is commonly the case for rivers and streams, this relationship can be  
 335 computed if the water depth  $d$  is known:

336 
$$F = \frac{v}{c} = \frac{v}{\sqrt{gd}} \quad (6).$$

337 Combining equation 3, 4, and 6 yields then a simple expression where:

338 
$$F = \sqrt{8 \frac{S}{f}} \quad (7).$$

339 This expression states that the flow regime, expressed here by the Froude number  $F$ ,  
 340 depends on two partly non-related variables. In particular, for a given bed friction  $f$ ,  
 341 which depends on the bed roughness (Ferguson, 2007), upper flow regime conditions  
 342 tend to establish for steep channels. Contrariwise, lower regime flows may occur in a  
 343 steep environment where poorly sorted material exerts a large resistance on the flow,  
 344 thereby reducing the flow velocity and hence the Froude number. Accordingly, where  
 345 the entrainment of sediment particles can be expressed through the Shields (1936)  
 346 variable  $\phi$ , the dependency of  $F$  on the channel gradient  $S$  can be computed through the  
 347 combination of equations 2, 3, 5 and 7:

348 
$$F = \sqrt{\frac{S}{\left(\frac{\rho S}{\phi(\rho_s - \rho)}\right)^2 * a_2^{-2} + \left(\frac{\rho S}{\phi(\rho_s - \rho)}\right)^{1/3} * a_1^{-2}}} \quad (8).$$

geo Uni Bern 30.7.2018 22:11  
Deleted: 6

geo Uni Bern 30.7.2018 22:11  
Deleted: 6

geo Uni Bern 30.7.2018 22:11  
Deleted: 1

geo Uni Bern 30.7.2018 22:11  
Deleted: 6

geo Uni Bern 30.7.2018 22:11  
Deleted: .

geo Uni Bern 30.7.2018 22:11  
Deleted: 7

geo Uni Bern 30.7.2018 22:11  
Deleted: 5,

geo Uni Bern 30.7.2018 22:11  
Deleted: 7

geo Uni Bern 30.7.2018 22:11  
Deleted: 8

geo Uni Bern 30.7.2018 22:11  
Deleted: ,

geo Uni Bern 30.7.2018 22:11  
Deleted: , for channel forming floods

geo Uni Bern 30.7.2018 22:11  
Deleted: 4, 6

geo Uni Bern 30.7.2018 22:11  
Deleted: 8, where

geo Uni Bern 30.7.2018 22:11

Deleted:  $F = \frac{S}{\left(\frac{\rho S}{\phi(\rho_s - \rho)}\right)^2}$   
.....(9).

364 Alternatively, also during channel forming floods, an expression where the Froude  
365 number depends on the bed roughness  $D_{84}/d$  only can be achieved through the  
366 combination of equations 2, 3, and 7:

$$367 \quad F = \sqrt{\frac{8 * \phi(\rho_s - \rho) * D_{84}}{\rho * f * d}} \quad (9).$$

368 We thus used equations 8 and 9 to calculate the Froude numbers at the incipient motion  
369 of the  $D_{84}$  grain sizes. We then compared these results with data from modern streams  
370 and stratigraphic records.

#### 372 2.4 Collection of data from modern streams and stratigraphic records

373 We used observations about clast arrangements in gravelly streams in Switzerland. We  
374 paid special attention to the occurrence of clast imbrications, as we hypothesize that this  
375 fabric may document the occurrence of upper flow regimes (Figure 1) upon sedimentation  
376 and gravel bar migration. We selected those sites for which Litty and Schlunegger (2017)  
377 reported grain size data (Table 1). At these locations, we explored multiple gravel bars for  
378 the occurrence or absence of clast imbrications over a reach of several hundreds of  
379 meters. We then determined a mean energy gradient over a c. 500 m-long reach, which  
380 we calculated from topographic maps at scales 1:10'000.

381 The selected streams are all situated around the Central Alps (Figure 2), have various  
382 upstream drainage basins and different source rock lithologies (Spicher, 1980) and grain  
383 size distributions. At sites where grain size data has been collected, the ratio between the  
384 clasts' medium  $b$ - and longest  $a$ -axes are constant and range between 0.67 and 0.72  
385 irrespective of the grain size distribution in these streams (Litty and Schlunegger, 2017).  
386 For these sites, we calculated the bed roughness  $D_{84}/d$  at the incipient motion of the  $D_{84}$ .  
387 Here, related water depths  $d$  were determined through the combination of equations (2)  
388 and (3), and using the channel gradient  $S$  at these sites.

389 The Swiss Federal Office for the Environment (FOEN) estimated the Froude numbers for  
390 various flood magnitudes of selected streams situated on the northern side of the Swiss  
391 Alps (Spreafico et al., 2001; see Figure 2 for location of sites). These estimates are based  
392 on flow velocities, flow depths and cross-sectional geometries of channels. The authors of  
393 this study also determined the corresponding channel gradient over a reach of several  
394 hundred meters. Because we will calculate the dependency of the Froude number on the  
395 channel gradient and the thresholds for the entrainment of sediment, expressed through  
396 different  $\phi$ -values, we will use the Spreafico et al. (2001) dataset to constrain the range of  
397 possible  $\phi$ -values for streams in Switzerland.

398 We finally identified possible relationships between channel gradient, bed roughness, and  
399 the occurrence of clast imbrications from stratigraphic records. We focused on the Late  
400 Oligocene suite of alluvial megafan conglomerates (Rigi and Thun sections, Figure 2)

geo Uni Bern 30.7.2018 22:11  
Deleted: , 4

geo Uni Bern 30.7.2018 22:11  
Deleted: 8

geo Uni Bern 30.7.2018 22:11

Deleted:  $F = \sqrt{\frac{8 * \phi(\rho_s - \rho) * D_{84}}{\rho * f * d}}$   
.....(10).....

geo Uni Bern 30.7.2018 22:11  
Deleted: use

geo Uni Bern 30.7.2018 22:11  
Deleted: 9

geo Uni Bern 30.7.2018 22:11  
Deleted: 10

geo Uni Bern 30.7.2018 22:11  
Deleted: compare

geo Uni Bern 30.7.2018 22:11  
Formatted: Font:Not Italic

geo Uni Bern 30.7.2018 22:11  
Deleted: is likely to

geo Uni Bern 30.7.2018 22:11  
Deleted: alternating shifts in

geo Uni Bern 30.7.2018 22:11  
Deleted: ), and

geo Uni Bern 30.7.2018 22:11  
Deleted: compared

geo Uni Bern 30.7.2018 22:11  
Deleted: observed fabric with the local

geo Uni Bern 30.7.2018 22:11  
Deleted: over a reach of c. 500 m

geo Uni Bern 30.7.2018 22:11  
Deleted:  $D$

geo Uni Bern 30.7.2018 22:11  
Deleted: are

geo Uni Bern 30.7.2018 22:11  
Deleted: 3

geo Uni Bern 30.7.2018 22:11  
Deleted: 4

419 deposited at the proximal border of the Swiss Molasse basin. For these conglomerates,  
420 Garefalakis and Schlunegger (2018) and Schlunegger and Norton (2015) collected data  
421 about the depth and gradient of palaeo-channels, and information about the grain size  
422 distribution along c. 3000 to 3600 m-thick sections (Table 1). We returned to these  
423 sections and examined c. 50 sites for the occurrence of clast imbrications along the  
424 conglomerate suites.

### 426 3 Results

#### 427 3.1 Calculation of flow regimes as a function of bed roughness and channel gradient

428 We calculated the Froude numbers  $F$  for different values of channel gradient  $S$ , bed  
429 roughness  $D_{84}/d$  and threshold conditions  $\phi$  for the incipient motion of material, and we  
430 compared these results with observations from modern streams and stratigraphic records.

431 We avoided calculation of the Froude numbers for slopes steeper than  $1.4^\circ$  because  
432 channels tend to adapt a step-pool geometry in their thalwegs (Whipple, 2014), for which  
433 our simple calculations might no longer apply. We set the thresholds for critical flow  
434 conditions to a Froude number  $F=0.9$ , which is consistent with estimations for the  
435 formation of upper flow regime bedforms by Koster (1978). Calculations were initially  
436 carried out using a Shields variable of  $\phi=0.0495\approx 0.05$ , as this value has commonly been

437 used in a large number of studies (see above). The results reveal that the Froude number  
438 increases with steeper channels (Figure 3A) and reaches the field of critical conditions for  
439  $\sim 0.5^\circ$  slopes. The values reach a maximum of nearly 1 where channel gradients are  
440 between  $\sim 0.8^\circ$ – $1^\circ$ . Froude numbers then slightly decrease for channels steeper than  $1^\circ$   
441 and finally reach a value of 0.9 for gradients  $>1.2^\circ$ . In the case of greater thresholds for the  
442 incipient motion of clasts, which is expressed through a larger Shields (1936) variable of  
443  $\phi=0.06$ , flows adapt supercritical conditions for channels steeper than  $\sim 0.4^\circ$ . For cases  
444 where the thresholds for the entrainment of the material are less (expressed here through  
445 a lower Shields (1936) variable of  $\phi=0.03$ ), streams remain in the lower flow regime.

446 The Froude number pattern is quite similar for increasing bed roughness (Figure 3B). For  
447 threshold conditions expressed through a Shields (1936) variable  $\phi=0.0495\approx 0.05$ , the  
448 Froude numbers increase with higher relative bed roughness. Supercritical conditions are  
449 reached for a bed roughness of c. 0.1, after which the Froude numbers decrease with  
450 greater roughness. At larger threshold conditions for sediment entrainment, expressed  
451 through a Shields variable  $\phi=0.06$ , upper flow regime conditions might prevail for bed  
452 surface roughness values between 0.06 and 0.5. Smaller and larger roughness values will  
453 keep the flow in the lower regime. Contrariwise, the stream will not shift to the upper  
454 regime for  $\phi$ -values as low as 0.03. Note that the consideration of the full range of  
455 roughness-layer and skin friction effects, expressed through the coefficients  $a_1$  and  $a_2$  in  
456 equation (8), shifts the pattern of Froude values to lower and higher values. But this will not

geo Uni Bern 30.7.2018 22:11  
Deleted: paleo

geo Uni Bern 30.7.2018 22:11  
Formatted: Font:Not Italic

geo Uni Bern 30.7.2018 22:11  
Deleted: at

geo Uni Bern 30.7.2018 22:11  
Deleted: the  $D_{84}$  grain sizes

geo Uni Bern 30.7.2018 22:11  
Deleted: to calculate

geo Uni Bern 30.7.2018 22:11  
Deleted:  $\phi =$

geo Uni Bern 30.7.2018 22:11  
Deleted: 047, which appears appropriate for  $D_{84}$  grain sizes.

geo Uni Bern 30.7.2018 22:11  
Deleted: Number

geo Uni Bern 30.7.2018 22:11  
Deleted: reach

geo Uni Bern 30.7.2018 22:11  
Deleted: a

geo Uni Bern 30.7.2018 22:11  
Deleted: flow

geo Uni Bern 30.7.2018 22:11  
Deleted: poorly sorted beds

geo Uni Bern 30.7.2018 22:11  
Deleted:  $D_{84}$

geo Uni Bern 30.7.2018 22:11  
Deleted:  $\phi =$

geo Uni Bern 30.7.2018 22:11  
Deleted: 047

geo Uni Bern 30.7.2018 22:11  
Deleted: gravel beds with poorly sorted clasts and thus for low threshold conditions for the entrainment of material (Shields variable  $\phi=0.03$ ).

476 alter the general finding that upper flow regime conditions at the incipient motion of gravels  
477 might be expected for channel gradients  $S$  that are steeper than  $0.5^\circ \pm 0.1^\circ$ , and for a bed  
478 roughness  $D_{84}/d$  greater than  $\sim 0.06$ .

479 We also calculated the Froude numbers for a Shields variable of  $\phi = 0.1$ , because  
480 observations have shown that thresholds for the entrainment of sediment particles may  
481 increase with steeper channels (Mueller et al., 2005; Ferguson, 2012). This might be an  
482 exaggeration (Lamb et al., 2008), but will give an upper bound for the dependence of the  
483 Froude number on the Shields variable. We additionally considered the case where the  
484 Shields (1936) variable depends on the channel gradient  $S$  through  $\phi = 2.81 * S + 0.021$   
485 (Mueller et al., 2005). These relationships have been established using bed load rating  
486 curves, which are based on field surveys in mountainous streams in North America and  
487 England. We found that the flows shift to critical conditions for channels steeper than  
488 between  $0.5^\circ$  and  $0.6^\circ$  (slope dependent  $\phi$ ) and for a bed roughness  $> 0.04$  ( $\phi = 0.1$ ).

489 In summary, the calculations predict that water flow may shift to upper flow regime  
490 conditions for: (i)  $\phi$ -values larger than 0.05; (ii) slopes steeper than  $\sim 0.5^\circ \pm 0.1^\circ$ ; and (iii)  
491 relative bed roughness values greater than  $\sim 0.06 \pm 0.01$ .

### 493 3.2 Estimates of $\phi$ -values from modern streams in the Central Alps

494 Spreafico et al. (2001) estimated the Froude numbers for various streams situated on the  
495 northern side of the Swiss Alps. Related values range between 0.2 and 1.1 and generally  
496 increase together with channel gradients (vertical bars on Figure 3A). The surface  
497 expressions of the flows particularly of the Birse and Thur streams (labeled as  $b$  and  $t$  on  
498 Figure 3A) are characterized by multiple hydraulic jumps (Spreafico et al., 2001, p. 71 and  
499 p. 77). Therefore, the inferred small Froude numbers (between 0.6 and 0.9) of these  
500 streams have to be treated with caution.

501 The Froude number estimates by Spreafico et al. (2001) disclose a large scatter in the  
502 relationship to the channel gradient (Figure 3A, vertical bars). This can partially be  
503 explained by site-specific differences in bed roughness, which are related to anthropogenic  
504 corrections and constructions (Spreafico et al., 2001). Nevertheless, the comparison  
505 between these data and the results of our calculations reveal that the entire range of  $\phi$ -  
506 values between 0.03 and 0.1 has to be taken into account for the hydrological conditions in  
507 the streams surrounding the Swiss Alps (Figure 3A). This also implies that the selection of  
508 a threshold, expressed by the  $\phi$ -value, warrants a careful justification, which we present in  
509 the discussion.

### 511 3.3 Data about the occurrence or absence of clast imbrications from modern streams

512 Here, we present evidence for imbrications and non-imbrications from modern rivers,  
513 and we relate these observations to channel slope (Figure 4A) and bed roughness

geo Uni Bern 30.7.2018 22:11

Deleted: ).

geo Uni Bern 30.7.2018 22:11

Deleted: variable

geo Uni Bern 30.7.2018 22:11

Deleted: ).

geo Uni Bern 30.7.2018 22:11

Deleted: streams where channel gradients are

geo Uni Bern 30.7.2018 22:11

Deleted: °,

geo Uni Bern 30.7.2018 22:11

Deleted: where

geo Uni Bern 30.7.2018 22:11

Deleted: exceeds a value of

geo Uni Bern 30.7.2018 22:11

Deleted: Data

geo Uni Bern 30.7.2018 22:11

Formatted: Font:Not Italic

geo Uni Bern 30.7.2018 22:11

Formatted: Font:Not Italic

geo Uni Bern 30.7.2018 22:11

Deleted: Grain size,

524 (Figure 4B). Data on grain size, stream runoff and channel morphology are available for  
525 several rivers in the northern, the central and the southern part of the Swiss mountain belt.  
526 These streams are situated both in the core of the Alps and the foreland. The bedrock-  
527 geology of their headwaters includes the entire range of lithologies from sedimentary units  
528 to schists, gneisses and granites. In the same sense, the streams cover the full range of  
529 water sources in their headwaters including glaciers and surface runoff. Except for the  
530 Maggia River between the sites Bignasco and Losone (Figure 2), all streams are  
531 channelized, and the rivers generally flow in a bed that is laterally confined by artificial  
532 riverbanks. These are either made up of concrete walls or oversized boulders. In this  
533 context, information about the hydrographs, grain size and the results of the shear stress  
534 calculations consider the time after these constructions have been made.

#### 536 Channel morphologies

537 The thalweg of the streams meanders between the artificial walls within a 20 to 50 m-wide  
538 belt. Flat-topped longitudinal bars that are several tens of meters long and that emerge up  
539 to 1.5 m above the thalweg are situated adjacent to the artificial riverbanks on the slip-off  
540 slope of these meanders. They evolve into subaquatic transverse bars, or riffles, farther  
541 downstream where the thalweg shifts to the opposite channel margin. Channels are  
542 deepest and flattest along the outer cutbank side of the meanders and in pools  
543 downstream of riffles, respectively. The thalweg then steepens where it crosses the  
544 transverse bars and riffles. This is also the location where some streams show evidence  
545 for standing waves with wavelengths >5 m (e.g., at Reuss, Figure 5). Standing waves have  
546 also been encountered in the Waldemme River at Littau (Figure 6B) when water runoff at  
547 that particular site was c. 100 m<sup>3</sup>/s and when rumbling sounds suggested that clasts were  
548 rolling or sliding. The streams thus display a complex pattern where channel depths, flow  
549 velocities and possibly also hydrological regimes alternate over short distances of tens to  
550 hundreds of meters. These arrangements of channel-bar pairs and particularly their  
551 positions within the channel belt has been stable over the past years as the locations of  
552 the gravel bars are still the same as the ones reported by Litty and Schlunegger (2016).

#### 554 Streams with evidence for clast imbrication

555 Inspections of gravel bars have shown clear evidence for imbrications in the Glenner, the  
556 Landquart, the Verzasca, and the Waldemme rivers (Table 1). In these streams, channel  
557 gradients range between 0.6° (Waldemme) and 1.2° (Glenner) (Figure 4A). The sizes of  
558 the  $D_{84}$  range between 3 cm (Waldemme) and 12 cm (Glenner). The gravel lithology  
559 includes the entire variety from sedimentary (Waldemme) to crystalline constituents  
560 (Glenner, Landquart, Verzasca). The inferred bed roughness at the incipient motion of the  
561  $D_{84}$  includes the range between c. 0.125 (Waldemme) and 0.31 (Glenner) (Figure 4B). In

geo Uni Bern 30.7.2018 22:11

Deleted: and stream runoff data

geo Uni Bern 30.7.2018 22:11

Deleted: streams

geo Uni Bern 30.7.2018 22:11

Deleted: Alps

geo Uni Bern 30.7.2018 22:11

Deleted: rivers

geo Uni Bern 30.7.2018 22:11

Deleted: As mentioned above, the

geo Uni Bern 30.7.2018 22:11

Deleted: then

geo Uni Bern 30.7.2018 22:11

Deleted: these

geo Uni Bern 30.7.2018 22:11

Deleted: the stream shows

geo Uni Bern 30.7.2018 22:11

Deleted: Figures 2, 4A

geo Uni Bern 30.7.2018 22:11

Deleted: at

geo Uni Bern 30.7.2018 22:11

Deleted: Figures 2, 4B

geo Uni Bern 30.7.2018 22:11

Deleted: 3C). In addition, the

geo Uni Bern 30.7.2018 22:11

Deleted: 3D).

575 [these streams, bars with imbricated clasts alternate with pools over a reach of several](#)  
576 [hundreds of meters.](#)

577 At Maggia, Reuss and Waldemme Littau, the largest clasts are arranged as triplets or  
578 quadruplets of imbricated constituents within generally flat lying to randomly-oriented finer  
579 grained sediment particles. The density of these arrangements ranges between 5 groups  
580 per 10 m<sup>2</sup> (Maggia Bignasco, Maggia Losone) to c. 10 groups per 10 m<sup>2</sup> (Maggia Visletto,  
581 Reuss, Waldemme Littau e.g. Figure [6D](#)). The channel gradients at these sites span the  
582 range between c. 0.3 and 0.6°, and the  $D_{84}$  clasts are between 3 and 9 cm large (Reuss  
583 and Maggia Visletto). Accordingly, the relative bed roughness at the incipient motion of the  
584  $D_{84}$  ranges between 0.07 and 0.16.

585 [At all sites mentioned above, clasts on subaquatic and subaerial gravel bars are generally](#)  
586 [arranged as well-sorted and densely packed clusters, possibly representing incipient](#)  
587 [bedforms \(e.g., Figure 6D\). In most cases, grains imbricate behind an outsized clast, which](#)  
588 [usually delineates the front of imbricated arrangements of sediment particles. In addition,](#)  
589 [the lowermost 10-20% part of most of the large clasts is embedded, and thus buried, in a](#)  
590 [fine-grained matrix, which was most likely deposited during the waning stage of a flood.](#)  
591 [Isolated, non-buried clasts that are flat lying on their a-b-planes do occur but are less](#)  
592 [frequent than embedded clasts or constituents arranged in clusters. The inclination dip of](#)  
593 [the a-b-planes ranges between c. 20-40° \(Figure 6D\). Finally, streams with clast](#)  
594 [imbrications display surface expressions, which point to an upper flow regime during low](#)  
595 [\(e.g., Reuss, Figure 5B\) and high-water stages \(e.g., Waldemme, Figure 6B\).](#)

#### 596 [Streams with little or no evidence for clast imbrication](#)

598 Gravel bars within the Emme [stream](#) are made up of generally flat lying gravels and  
599 cobbles. [A small tilt of <10° of a-b-planes occurs where individual clasts slightly overlap](#)  
600 [each other, similar to a shingling arrangement of particles.](#) This is particularly the case in  
601 pools and on the upstream stoss-side of longitudinal and transverse bars where channel  
602 gradients are flat. [Also in the Emme River, clast imbrications occur in places only where](#)  
603 [gravel bars have steep downstream slip faces, which are mainly observed at the end of](#)  
604 [transverse bars. At sites where imbrication is absent, most of the clasts are lying flat on](#)  
605 [their a-b-planes, and embedding by finer-grained material is less frequently observed than](#)  
606 [in streams with clast imbrications. The channel gradient is less than 0.5°, and the size of](#)  
607 [the  \$D\_{84}\$  measures 2 cm. The bed roughness of this stream, calculated for the incipient of](#)  
608 [motion of the 84<sup>th</sup> grain size percentile, ranges between 0.07 and 0.10. Finally, the flow](#)  
609 [displays a smooth surface expression during low- and high-water stages \(Spreafico et al.,](#)  
610 [2001, p. 53\), which is a characteristic evidence for lower flow regime conditions.](#)

611 [The channel morphology of the Sense River differs from that of the Emme stream in the](#)  
612 [sense that bedrock reaches alternate with alluvial segments over a wavelength of 100-200](#)  
613 [meters and more. Alluvial segments are flat \(c. 0.3°\) and host lateral and transverse gravel](#)

geo Uni Bern 30.7.2018 22:11

Deleted: 4D

geo Uni Bern 30.7.2018 22:11

Deleted: and Sense (Figure 4C) streams

geo Uni Bern 30.7.2018 22:11

Deleted: (Table 1; Figures 3C, 3D). In both streams

geo Uni Bern 30.7.2018 22:11

Deleted: Also

geo Uni Bern 30.7.2018 22:11

Deleted: these

geo Uni Bern 30.7.2018 22:11

Deleted: ,

geo Uni Bern 30.7.2018 22:11

Deleted: gradients are

geo Uni Bern 30.7.2018 22:11

Deleted: °. The sizes

geo Uni Bern 30.7.2018 22:11

Deleted: measure between

geo Uni Bern 30.7.2018 22:11

Deleted: (Emme) and 6 cm (Sense).

geo Uni Bern 30.7.2018 22:11

Deleted: these streams

geo Uni Bern 30.7.2018 22:11

Deleted: .



627 bars where the  $D_{84}$  measures 6 cm. On top of these bars, gravels are generally lying flat  
628 on their  $a$ - $b$ -planes (Figure 6C). Imbrications are observed where some of these gravels  
629 are overlapping each other, resulting in a dip angle of 10-20°. Contrariwise, bedrock  
630 reaches (site  $S'$  on Figure 4A) that form distinct steps in the thalweg are up to 0.5° steep  
631 and partly covered by subaquatic longitudinal bars (Figure 1B) where imbricated clasts  
632 alternate with flat-lying grains at the meter scale. The channel bed surface is generally  
633 well-sorted and well-armored where clasts are either interlocked, partly isolated, and also  
634 rooted in a finer-grained matrix, as a photo of a subaquatic longitudinal bar shows (Figure  
635 6A). At these sites, upper flow regime segments laterally change to lower flow regime  
636 reaches over short distances of a few meters (Figure 1B). While we have made this  
637 observation during low water stages only, it is very likely that sub- and supercritical flows  
638 also change during flood stages over short distances, as various examples of Alpine  
639 streams show (Spreafico et al., 2001).

641 3.4 Data about the occurrence or absence of clast imbrications from stratigraphic  
642 records

643 Here, we calculated patterns of bed roughness and related channel gradients and explored  
644 c. 50 conglomerate sites for the occurrence or absence of clast imbrications. We used  
645 published data about channel depth  $d$ , surface gradients  $S$  and information about the  
646 pattern of the  $D_{84}$ , which have been reported from the Late Oligocene alluvial megafan  
647 conglomerates at Rigi (47°03'N / 8°29'E) and Thun (46°46'N / 7°44'E) situated in the  
648 Molasse foreland basin north of the Alpine orogen (Figure 2, Table 1). The depositional  
649 evolution of these conglomerates has been related to the rise of the Alpine mountain belt  
650 and the associated erosional history of this orogen (Kempf et al., 1999; Schlunegger and  
651 Castellort, 2016).

652 The deposits at Rigi are c. 3600 m thick and made up of an alternation of conglomerates  
653 and mudstones (Stürm, 1973) that were deposited between 30 and 25 Ma according to  
654 magneto-polarity chronologies and mammal biostratigraphic data (Engesser and Kälin,  
655 2017). Garefalakis and Schlunegger (2018) subdivided this alternation of conglomerates  
656 and mudstones into four segments labeled as  $\alpha$  through  $\delta$ . The lowermost segments  $\alpha$   
657 and  $\beta$  are an alternation of mudstones and conglomerate beds and were deposited by  
658 gravelly streams (Stürm, 1973). According to Garefalakis and Schlunegger (2018), the  
659 depositional area was characterized by a low surface slope ranging between  $0.2 \pm 0.06^\circ$   
660 and  $0.4 \pm 0.2^\circ$ . Channel depths span the range between 1.7 and 2.5 m, and the  $D_{84}$  values  
661 are between 2 and 6 cm. These measurements result in bed roughness values between  
662 0.02 and 0.05. Except for one site, we found no imbrications in outcrops of  $\alpha$  and  $\beta$  units  
663 (Figures 4, 7A).

664 The top of the Rigi section, referred to as segments  $\gamma$  and  $\delta$  by Garefalakis and

geo Uni Bern 30.7.2018 22:11

Formatted: Font:Not Italic

geo Uni Bern 30.7.2018 22:11

Formatted: Font:Not Italic

geo Uni Bern 30.7.2018 22:11

Formatted: Widow/Orphan control, Adjust space between Latin and Asian text, Adjust space between Asian text and numbers

geo Uni Bern 30.7.2018 22:11

Moved (insertion) [1]

geo Uni Bern 30.7.2018 22:11

Deleted: We calculated patterns of bed roughness and related channel gradients and explored c.

geo Uni Bern 30.7.2018 22:11

Moved up [1]: 50 conglomerate sites for the occurrence or absence of clast imbrications.

geo Uni Bern 30.7.2018 22:11

Deleted: where channels were laterally bordered, and thus confined, by a floodplain

geo Uni Bern 30.7.2018 22:11

Deleted: We

geo Uni Bern 30.7.2018 22:11

Deleted: at 13 sites

geo Uni Bern 30.7.2018 22:11

Deleted: 3C, 3D, 4E), and only one conglomerate outcrop displayed evidence for clast imbrications.

679 Schlunegger (2018), is an amalgamated stack of conglomerate beds deposited by non-  
680 confined braided streams (Stürm, 1973). Garefalakis and Schlunegger (2018) inferred  
681 values between  $0.65 \pm 0.2^\circ$  and  $0.9 \pm 0.4^\circ$  for the palaeo-gradient of these rivers (Table 1).  
682  $D_{84}$  values range between 6 and 12 cm, and palaeo-channels were c. 1.2 m deep. This  
683 yields a relative bed roughness between c. 0.05 and 0.12. Interestingly, a large number of  
684 conglomerate sites within the segments  $\gamma$  and  $\delta$  display evidence for clast imbrications in  
685 outcrops parallel to the palaeo-discharge direction (Figures 4, 6B). In addition, some  
686 outcrops show sedimentary structures that correspond to cluster bedforms of imbricated  
687 clasts (C on Figure 7B). However, at all sites, the lateral extents of groups with imbricated  
688 clasts are limited to widths of 1-2 meters. Please refer to Garefalakis and Schlunegger  
689 (2018) and their Figure 2 for location of sites displaying units  $\alpha$  through  $\delta$ .

690 The up to 3000 m-thick conglomerates at Thun are slightly younger, and the ages span the  
691 time interval between c. 26 and 24 Ma according to magneto-polarity chronologies  
692 (Schlunegger et al., 1996). Similar to the Rigi section, the conglomerates at Thun start with  
693 an alternation of conglomerates, mudstones and sandstones, which has been referred to  
694 as unit A. This suite is overlain by an up to 2000 m-thick amalgamated stack of  
695 conglomerate beds (unit B). Channel depths within unit A range between 3 to 5 m, and  
696 streams were between  $0.1^\circ$  and  $0.3^\circ$  steep. Channels in the overlying unit B were  
697 shallower and between 1.5 and 3 m deep. Stream gradients varied between  $0.4^\circ$  and  $1^\circ$ ,  
698 depending on the relationships between inferred water depths and maximum clast sizes  
699 (Schlunegger and Norton, 2015). In outcrops parallel to the palaeo-discharge direction,  
700 sequences with imbricated clasts have only been found in unit B where palaeo-channel  
701 slopes were steeper than  $0.4^\circ$  (Figure 4A). Similar to the Rigi section, the lateral extents of  
702 groups with imbricated clasts are limited to widths of a few meters only. No data is  
703 available for computing the  $D_{84}$  grain size, with the consequence that we cannot estimate  
704 the bed roughness for the Thun conglomerates. Please see Schlunegger and Norton  
705 (2015) for location of sites where units A and B are exposed.

706 Similar to the modern examples, imbricated clasts form a well-sorted cluster and  
707 commonly include the largest constituents of a gravel bar. In most cases, clasts imbricate  
708 behind an outsized constituent, which usually delineates the front of an imbricated  
709 arrangement of clasts (Figure 7B).

## 711 **4 Discussion**

### 712 **4.1 Selection of preferred boundary conditions**

713 Our calculations reveal that the results are strongly dependent on: (i) the selection of  
714 values for the Shields variable  $\phi$ ; (ii) the way of how we consider variations in slope  $S$  at  
715 the bar and reach scales, and (iii) the consideration of flood magnitudes which either result  
716 in the motion of individual sediment particles or the alteration of the shape of an entire

geo Uni Bern 30.7.2018 22:11

Deleted: paleo

geo Uni Bern 30.7.2018 22:11

Deleted: paleo

geo Uni Bern 30.7.2018 22:11

Deleted: (Figures 3D, 4F).

geo Uni Bern 30.7.2018 22:11

Deleted: this section

geo Uni Bern 30.7.2018 22:11

Deleted: paleo

geo Uni Bern 30.7.2018 22:11

Deleted: 3C

geo Uni Bern 30.7.2018 22:11

Deleted: .

724 channel (channel forming floods). This section is devoted to justify the selection of our  
725 preferred boundary conditions.

726  
727 *Thresholds regarding channel forming floods versus incipient motion of individual clasts*

728 We constrained our calculations on the incipient motion of individual clasts and used  
729 equation (1a) for all other considerations. This approach might be perceived as a large  
730 contrast to the hydrological conditions during channel forming floods where thresholds for  
731 the evacuation of sediment are up to 1.2 times larger, as theoretical and field-based  
732 analyses and have shown (Parker, 1978; Philips and Jerolmack, 2016; Pfeiffer et al.,  
733 2017). Nevertheless, the consequences on the outcome of our calculations are minor, at  
734 least when the Froude number dependencies on the slope and bed roughness parameters  
735 are considered. In fact, a 1.2-times larger threshold will increase the  $\phi$ -values (equation  
736 1b) to the range between 0.036 and 0.072. However, as illustrated in Figure 3, this will not  
737 change the general pattern. In addition, while channel forming floods are mainly  
738 associated with equal mobility of a large range of sediment particles, the formation of an  
739 imbricated fabric involves the clustering of individual clasts only. We use these arguments  
740 to justify our preference for using equation 1a (incipient motion of clasts) rather than  
741 equation 1b (channel forming floods).

742  
743 *Protrusion and hiding effects and consequences for the selection of  $\phi$ -values*

744 Larger bed surface grains, as is the case for most of the imbricated clasts, may exert lower  
745 mobility thresholds because of a greater protrusion and a smaller intergranular friction  
746 angle, as noted by Buffington and Montgomery (1997) in their review. Related  
747 consequences have been explored in experiments (e.g., Buffington et al., 1992) and  
748 through field-based studies, which were likewise complemented with experiments in the  
749 laboratory (Johnston et al., 1998). These studies resulted in the notion that the entrainment  
750 of the largest clasts (e.g., the  $D_{84}$ ) most likely requires lower flow strengths than the shift of  
751 median-sized sediment particles. As a consequence, while  $\phi$ -values might be as high as  
752 0.1 for the displacement of the  $D_{50}$  (Buffington et al., 1992), conditions for the incipient  
753 dislocation of large clasts could be significantly different. In particular, for clasts that are up  
754 to five times larger than the  $D_{50}$  (which corresponds to the ratio between the  $D_{84}$  and the  
755  $D_{50}$  of the Swiss data, Table 1), Buffington et al (1992) and also Johnston et al. (1998)  
756 predicted  $\phi$ -values that might be as low as 0.03 or even less. Related  $\phi$ -values, for  
757 instance, have indeed been applied for mountainous streams where the supply of  
758 sediment from the lateral hillslopes has been large (van der Berg and Schlunegger, 2012).  
759 Large sediment fluxes have been considered to result in a poor sorting and a low packing  
760 of the material, and thus in low thresholds particularly for the incipient motion of large clast

761 [\(Lenzi et al., 2006; van der Berg and Schlunegger, 2012\)](#). Our calculations predict that an  
762 [upper flow regime is very unlikely to establish at these conditions \( \$\phi\$ -value of 0.03\)](#).  
763 [However, we consider it unlikely that the formation of most of the imbrications, as we did](#)  
764 [encounter in the analyzed Alpine streams and in the stratigraphic record, were associated](#)  
765 [with thresholds as low as those proposed by e.g., Lenzi et al. \(2006\) and van der Berg and](#)  
766 [Schlunegger \(2012\)](#). We base our inference on the observation that the analyzed gravel  
767 [bars display an arrangement where large clasts are generally well sorted and densely](#)  
768 [packed, both on subaerial \(during low water stages\) and subaquatic bars. This results in a](#)  
769 [high interlocking degree of sediment particles within the bars we have encountered in the](#)  
770 [field. In addition, field inspections showed that the base of most of the large clasts,](#)  
771 [particularly those in subaquatic bars, are embedded and thus buried in finer grained](#)  
772 [material, and only very few clasts are lying isolated and flat on their \*a-b\*-planes. This](#)  
773 [implies that the fine-grained sediment particles have to be removed before these clasts](#)  
774 [can be entrained. In this case, hiding effects associated with  \$\phi\$ -values  \$>0.5\$  would possibly](#)  
775 [be appropriate for the prediction of material entrainment of the finer-grained sediments](#)  
776 [before the larger clasts can be shifted \(Buffington and Montgomery, 1997\). As a](#)  
777 [consequence, a dislocation of these clasts and thus a rearrangement of the sedimentary](#)  
778 [fabric most likely require that large thresholds have to be exceeded, which is mainly](#)  
779 [accomplished through high-discharge events with large flow strengths. We thus propose](#)  
780 [that the use of  \$\phi\$ -values of c. 0.05, which is commonly used for the entrainment of the  \$D\_{50}\$](#)   
781 [\(Paola and Mohring, 1996\), is also adequate for the calculation of the hydrological](#)  
782 [conditions associated with the fabric we have encountered in the field. We do](#)  
783 [acknowledge, however, that this hypothesis warrants a test with quantitative data, which](#)  
784 [we have not available. Please note that the low Froude numbers and thus the low  \$\phi\$ -values](#)  
785 [of 0.3 inferred for the Thur and the Birse streams might be underestimated, because](#)  
786 [photos that were taken during high stage flows of these streams display clear evidence for](#)  
787 [multiple hydraulic jumps over m-long reaches \(Spreafico et al., 2001, p. 71 and 77\)](#).

788

#### 789 *Variations in channel gradient at the bar and reach scales*

790 [Figure 3 shows that the results largely hinge on the values of  \$\phi\$  and  \$S\$ . We applied](#)  
791 [equation 3 while inferring a steady uniform flow and a bed slope, which is constant over a](#)  
792 [distance of 500 m. We did not consider any smaller-scale slope variations that are caused](#)  
793 [by downstream alternations of bars, riffles and pools as we lack the required quantitative](#)  
794 [information. This inference results in an energy slope, which is neither equal to the water](#)  
795 [surface slope nor to the bed slope. Such inequalities increase substantially when unsteady](#)  
796 [non-uniform super-critical flows and transitions are considered \(e.g., Figure 1A\), which is](#)  
797 [not fully described by equations 3 and 4, and which introduces a bias. These variations in](#)  
798 [channel floor morphologies are likewise not depicted in experiments either \(e.g., Buffington](#)

799 [et al., 1992; Powell et al., 2016](#)), which could partially explain the low  $\phi$ -values that result  
800 [from these studies. We justify our simplification because we are mainly interested in](#)  
801 [exploring whether supercritical flows are likely to occur for particular  \$\phi\$ - and channel](#)  
802 [gradient values.](#)

#### 804 4.2 Relationships between channel gradient, bed roughness and flow regime

805 We have found an expression where the Froude number  $F$ , and thus the change from the  
806 lower to the upper flow regime, depends on the channel gradient  $S$  and the bed roughness  
807  $D_{84}/d$  (eq. 7). This relationship also predicts that the controls of both parameters on the  
808 Froude number are to some extent independent from each other. Under these  
809 considerations, the similar pattern of how the Froude number  $F$  depends on channel  
810 gradient and bed roughness (Figure 3) appears unexpected. However, we note that we  
811 computed both relationships for the case of the incipient motion of the grain size percentile  
812  $D_{84}$ . This threshold is explicitly considered by equation 2, which we used as basis to derive  
813 an expression where the Froude number depends on the channel gradient or the bed  
814 roughness only. Therefore, it is not surprising that the dependencies of the Froude number  
815 on gradient and bed roughness follow the same trends. In addition, Blissenbach (1952),  
816 Paola and Mohring (1996) and also Church (2006) showed that channel gradient, water  
817 depth and grain size are closely related parameters during [the entrainment of sediment](#)  
818 [particles](#). In particular, channels with coarser grained gravel bars tend to be steeper and  
819 shallower than those where the bed material is finer grained (Church, 2006). In the same  
820 sense, also in steeper streams, bed roughness values tend to be larger than in flatter  
821 channels (Whipple, 2004). We use the causal relationships between these variables to  
822 explain the similarity in the patterns illustrated in Figures 3A and 3B.

823 The tendency towards lower Froude numbers for a channel gradient  $>1^\circ$  ( $\phi > 0.05$ ) and a  
824 bed roughness  $>0.3$  ( $\phi > 0.05$ ) is somewhat unexpected. We explain these trends through  
825 the [non-linear](#) relationships [between slope, water depth, the energy loss within the](#)  
826 [roughness-layer, and the velocity at the flow's surface,](#)

#### 828 4.3 The formation of imbrications in experiments

829 [Interpretations](#) of the [possible](#) linkages between hydrological conditions upon [material](#)  
830 [transport](#) and the [formation](#) of [imbrications](#) are hampered because [experiments have not](#)  
831 [been designed to explicitly explore these relationships. In addition, as noted by Carling et](#)  
832 [al. \(1992\), natural systems differ from the conditions in experiments because of the](#)  
833 [contrasts in scales. Nevertheless, it was possible to reproduce the formation of clast](#)  
834 [imbrications in subcritical flumes \(Carling et al., 1992\), or at least in the absence of any](#)  
835 [change in flow regime in many experiments. For instance, Qin et al. \(2013\) quantified the](#)  
836 [imbrications that resulted from the experiments by Aberle and Nikora \(2006\) where](#)

geo Uni Bern 30.7.2018 22:11  
Formatted: Font:Not Italic

geo Uni Bern 30.7.2018 22:11  
Deleted:  $D$

geo Uni Bern 30.7.2018 22:11  
Deleted: 8

geo Uni Bern 30.7.2018 22:11  
Deleted: Figures 3A and 3B

geo Uni Bern 30.7.2018 22:11  
Deleted: 3

geo Uni Bern 30.7.2018 22:11  
Deleted: channel forming floods.

geo Uni Bern 30.7.2018 22:11  
Deleted: 047

geo Uni Bern 30.7.2018 22:11  
Deleted: 047

geo Uni Bern 30.7.2018 22:11  
Deleted: denoted in equation 1, which states that shallower floods (lower  $d$ ) require steeper channels for the entrainment of the  $D_{84}$  clasts. The result is a lower surface velocity relative to the same bottom shear stress of a flow. This is the case because

geo Uni Bern 30.7.2018 22:11  
Deleted: has a relatively large effect on

geo Uni Bern 30.7.2018 22:11  
Deleted: if the water column is shallow. The same relationships are expected for a large bed roughness

geo Uni Bern 30.7.2018 22:11  
Deleted: Relationships between flow regimes and clast imbrications - ... [7]

geo Uni Bern 30.7.2018 22:11  
Deleted: clast imbrications with shifts from supercritical to subcritical flows. However, interpretations

geo Uni Bern 30.7.2018 22:11  
Deleted: fabric

geo Uni Bern 30.7.2018 22:11  
Deleted: gravel bars

geo Uni Bern 30.7.2018 22:11  
Deleted: related flume

geo Uni Bern 30.7.2018 22:11  
Deleted: are

geo Uni Bern 30.7.2018 22:11  
Deleted: available.

866 flows have been stationary. Carling et al. (1992) additionally showed that the shape of a  
867 clast has a strong control on the thresholds for incipient motion, the style of motion, and  
868 the degree of imbrication. A similar arrangement of clasts was formed in the experiments  
869 by Powell et al. (2016) and Bertin and Friedrich (2018), who reproduced imbrications with  
870 low Froude numbers between c. 0.55 and 0.9. Please note that we inferred these numbers  
871 from the experimental setup of these authors. Powell et al. (2016) additionally showed that  
872 the material can be entrained with  $\phi$ -values as low as 0.03, which is consistent with  
873 calculations of Froude numbers for some of the streams in Switzerland. Also during  
874 experiments, Johansson (1963) reported particle vibration before entrainment either  
875 through rolling or sliding. He noted that imbrication was formed at conditions, which  
876 corresponded to the lower flow regime during the flume experiments. Based on field  
877 observations, Sengupta (1966) reported examples where imbrication was most likely  
878 initiated by the development of current crescents around pebbles that were embedded in  
879 sand, and that these processes possibly occurred during lower regime flows. Such eddies  
880 preferentially develop at the upstream end of pebbles, which then leads to the winnowing  
881 of the fine grained sand at the upstream edge and the tilting of this particular clast.  
882 Additional sliding, pivoting and vibrating of these sediment particles might then result in the  
883 final imbrication. If this process occurs multiple times and affects the sand-gravel interface  
884 at various sites, then an armored bed with imbricated clasts can establish without the  
885 necessity of supercritical flows, or changes in flow regimes, as experimental results have  
886 shown (Aberle and Nikora, 2006; Haynes and Pender, 2007). Such a fabric may even form  
887 in response to prolonged periods of sub-threshold flows, as summarized by Ockelford and  
888 Haynes (2013). Finally, using flume experiments in a 0.3 m-wide, 4 m-long, recirculating  
889 tilting channel flume, Brayshaw (1984) was able to reproduce cluster bedforms with  
890 imbricated clasts during subcritical flows ( $F$ -numbers between 0.03 and 0.07).  
891 However, inspections of photos illustrating the experimental set up reveal that the surface  
892 grains are either flat lying on finer-grained sediments before their entrainment (Figure 3 in  
893 Powell et al., 2016), occur isolated on the ground (Figure 2.1b in Carling et al., 1992), or  
894 have a low degree of interlocking (Figure 3a in Lamb et al., 2017). Interestingly, the  
895 experiment by Buffington et al. (1992) followed a different strategy, where a natural bed-  
896 surface of a stream was peeled off with epoxy. They subsequently used this peel in the  
897 laboratory to approximate a natural channel bed surface (see their Figure 4), on top of  
898 which they randomly placed grains with a known size distribution. Buffington and co-  
899 authors then measured the friction angle of the overlying grains, based on which they  
900 calculated the critical boundary shear stress values  $\phi$ . In all experiments, the surface  
901 morphology of the sedimentary material is flat and lacks topographic variations, which we  
902 found as reach-scale alternations of riffles, transverse bars and pools in the field. The low  
903  $\phi$ -values of 0.03, which appears to be typical of bed surface conditions that develop in

904 laboratory flumes (Ferguson, 2012), as summarized by Powell et al. (2016), could possibly  
905 be explained by these conditions. Furthermore, and probably more relevant, the lengths of  
906 the experimental reaches are generally less and range between e.g., 4.0 meters  
907 (Brayshaw, 1984), 4.4 meters (Powell et al., 2016), 15 meters (e.g., Lamb et al., 2017) and  
908 even 20 meters (Aberle and Nikora, 2006). We acknowledge that in most experiments the  
909 variables have been normalized through an e.g., constant Reynolds or Froude number  
910 (Brayshaw, 1984). This normalization also includes the experimental  $D_{50}$ -grain sizes, which  
911 are very similar to those we have determined for our selected streams (Litty and  
912 Schlunegger, 2017). Nevertheless, we find it really hard to upscale some of the results  
913 associated with these experiments to our natural cases where standing waves of 1 m, and  
914 even between 5 and 8 meters lengths may occur (our Figures 1B, 5B, 6B), which are not  
915 reproducible in the experiments. In addition, Powell et al. (2016) observed that the water  
916 surface stayed relatively stable during their experiments, and that the flows were steady  
917 and uniform without hydraulic jumps. This contrasts to our natural cases where upper and  
918 lower flow regimes alternate over short distances even during low-stage flows. Finally,  
919 while winnowing of fine grained material, tilting of clasts and subsequent bed armouring  
920 might be a valuable mechanism for the explanation of imbrications during low stage flows  
921 in experiments, we consider it unlikely that these results can be directly translated to our  
922 field observations. We base our inference on two closely related arguments. First, our  
923 reported groups of imbricated clasts tend to be arranged as cluster bedforms (e.g., Figures  
924 6D, 7B), which rather form in response to selective deposition of large clasts (Brayshaw,  
925 1984) than selective entrainment of fine-grained material (Figure 6A). Second,  
926 observations (Berther, 2012) and calculations (Litty and Schlunegger, 2017) have shown  
927 that effective sediment transport in these streams is likely to occur on decadal time scales  
928 (and most likely much shorter; van der Berg and Schlunegger, 2012), at least for  
929 subaquatic bars. Sediment transport is then likely to occur over a limited reach only. This  
930 means that a large fraction of the shifted material per flood has a local source situated in  
931 the same river some hundreds of meters farther upstream where bars are also well  
932 armored. This possibly calls for large thresholds for the removal of clasts. In addition, on  
933 subaerial bars, waning stages of floods result in the deposition of fine-grained material and  
934 not in the winnowing of sand, as our observations have shown. Accordingly, while low  
935  $\phi$ -values and thus a lower flow regime might be appropriate for predicting the entrainment  
936 of the sediment particles in experiments, greater thresholds and thus larger  $\phi$ -values are  
937 likely to be appropriate for our natural examples for the reasons we have explained in  
938 above.

939  
940 4.4 Possible relationships between flow regimes and clast imbrications based on field  
941 observations

942 Here, we provide evidence for proposing that clast imbrications can be linked with  
 943 supercritical flows provided that the gravel bars form a well-sorted arrangement of densely  
 944 packed particles with a clast-supported fabric, as we have encountered in our streams. We  
 945 sustain our inferences with (i) published examples from natural environments; (ii) our  
 946 observations from Swiss streams; and (iii) the results of our calculations.  
 947 For the North Saskatchewan River in Canada, Shaw and Kellerhals (1977) reported gravel  
 948 mounds on a lateral gravel bar, which have a regular spacing between 2 and 3 meters and  
 949 a relatively flat top. Shaw and Kellerhals considered these bedforms as antidunes, which  
 950 might have formed in the upper flow regime. Also in modern gravelly streams, transverse  
 951 ribs, which are a series of narrow, current-normally orientated accumulations of large  
 952 clasts, were considered as evidence for the deposition either under upper flow regime  
 953 conditions, or in response to upstream-migrating hydraulic jumps (e.g., Koster, 1978; Rust  
 954 and Gostin, 1981). Koster (1978) additionally reported that these bedforms are associated  
 955 with clast imbrications (Figure 2 in Koster, 1978). Alexander and Fielding (1997) found  
 956 modern gravel antidunes with well-developed clast imbrications in the Burdekin River,  
 957 Australia. Finally, Taki and Parker (2005) reported cyclic steps of channel floor bedforms  
 958 with wave-lengths that are 100–500 times larger than the flow thickness. These bedforms  
 959 most likely represent chute-and-pool configurations (Taki and Parker, 2005), which could  
 960 have formed in response to alternations of upper and lower flow regime conditions, as  
 961 outlined by Grant (1997). In such a situation, the upstream flow on the stoss-side of the  
 962 bedform may experience a reduction of the flow velocity, with the effect that the flow may  
 963 shift to subcritical conditions. This could be associated with a hydraulic jump and a drastic  
 964 reduction of the flow velocity and thus with a drop of shear stresses (Figure 1A). In gravelly  
 965 streams, such a situation could result in the deposition of clasts. In such a scenario, the  
 966 site where sediment accumulates most likely migrates upstream (Figure 3).  
 967 Inspections of modern gravel bars in the Central European Alps and of stratigraphic  
 968 records (Figure 4) reveal the occurrence of imbrications where channel slopes are steeper  
 969 than 0.4°-0.5°, and where the values of bed roughness exceed c. 0.06. The results of our  
 970 generic calculations (Figure 3) reveal that under these circumstances, flows might become  
 971 supercritical provided that  $\phi$ -values are greater than c. 0.05 (Figure 3). This is supported  
 972 by observations from the Waldemme and Reuss Rivers (slope >0.5°) during high stage  
 973 and low stage flows (Figures 5B and 6B) that provide evidence for standing waves and  
 974 thus supercritical flows. Contrariwise, the reach of the Emme River is flatter (slope <0.4°),  
 975 imbrications are largely absent, and flows generally occur in the lower flow regime  
 976 (Spreafico et al., 2001, p. 53). We thus propose that a channel gradient of c. 0.5° is critical  
 977 for both the formation of clast imbrications and possibly also for the establishment of  
 978 supercritical flows. Based on these relationships, we also suggest that the generation of  
 979 imbrications may be associated with upper flow regime conditions.

geo Uni Bern 30.7.2018 22:11  
 Deleted: m

geo Uni Bern 30.7.2018 22:11  
 Deleted: is

geo Uni Bern 30.7.2018 22:11  
 Deleted: in

geo Uni Bern 30.7.2018 22:11  
 Deleted: 1

geo Uni Bern 30.7.2018 22:11  
 Deleted: most likely results

geo Uni Bern 30.7.2018 22:11  
 Deleted: We use these mechanisms to explain the formation of clast imbrications, which record an upstream migration of

geo Uni Bern 30.7.2018 22:11  
 Deleted: 5). Accordingly, the occurrence of clast imbrications might record alternating shifts from upper to lower flow regimes separated by hydraulic jumps, which will also migrate upstream as the construction of the imbricated fabric proceeds (Figure 5). We support this interpretation through our generic calculations (Figures 3A, 3B) in combination with observations from

geo Uni Bern 30.7.2018 22:11  
 Deleted: streams

geo Uni Bern 30.7.2018 22:11  
 Deleted: (Figure 3C)

geo Uni Bern 30.7.2018 22:11  
 Deleted: from

geo Uni Bern 30.7.2018 22:11  
 Deleted: 3D). For both observational datasets, we find gravel bars with imbricated clasts in streams with a

geo Uni Bern 30.7.2018 22:11  
 Deleted: >

geo Uni Bern 30.7.2018 22:11  
 Deleted: and a slope >0.5°, consistent with the theoretical predictions for the occurrence of

geo Uni Bern 30.7.2018 22:11  
 Deleted: (Figure 3). This



1009 | [The proposed](#) threshold slope is [consistent with](#) the results of previous work, where upper  
 1010 | flow regime bedforms such as transvers ribs have been described for e.g., the Peyto  
 1011 | Outwash (slope c. 1.09°), the Spring Creek (same slope; McDonald and Banerjee, 1971),  
 1012 | and the North Saskatchewan River (slope 0.52°; Dept. Mines and Tech. Survs., 1957).  
 1013 | [This is also in agreement with observations \(Mueller et al., 2005\) and the results of](#)  
 1014 | [theoretical work calibrated with data \(Lamb et al., 2008\). In particular, Mueller et al. \(2005\)](#)  
 1015 | [suggested that a  \$\phi\$ -value of c. 0.03 is suitable for slopes  \$<0.35^\circ\$ , while  \$\phi > 0.1\$  might be](#)  
 1016 | [more appropriate for the mobilization of coarse-grained sediment particles in channels](#)  
 1017 | [steeper than  \$1.1^\circ\$ .](#) [This might be an overestimate of the  \$\phi\$ -dependency of slope \(Lamb et](#)  
 1018 | [al., 2008\), but it does show that  \$\phi\$ -values larger than the commonly used  \$\phi\$ -values](#)  
 1019 | [between 0.04 and 0.05 might be appropriate where channels are steep \(see also Ferguson,](#)  
 1020 | [2012\). Finally,](#) Simons and Richardson (1960, p. 45) noted that flows rarely exceeded unity  
 1021 | Froude numbers over an extended period of time in a stream with erodible banks. We thus  
 1022 | use the conclusion of their discussion to explain the limited spatial extent of individual  
 1023 | ensembles of imbricated clasts in modern streams and stratigraphic records.

## 1025 | **5 Summary and conclusions**

1026 | We started with the hypothesis that the transport and deposition of coarse-grained  
 1027 | particles, and particularly the formation of an imbricated fabric, [may be](#) related to changes  
 1028 | in flow regimes. We then calculated the Froude number  $F$  at conditions of incipient motion  
 1029 | of coarse-grained bedload for various bed roughness and stream gradient values, and we  
 1030 | compared the results with data from modern streams and stratigraphic records. The results  
 1031 | suggest that imbricated clasts are likely to provide evidence for the occurrence of  
 1032 | supercritical conditions, particularly at sites where channel gradients are steeper than  $\sim 0.5^\circ$   
 1033 | [and where  \$\phi\$ -values are greater than c. 0.05.](#) We do acknowledge that our field-based  
 1034 | inferences are associated with large uncertainties regarding channel gradients and grain  
 1035 | size (Litty and Schlunegger, 2017), and that they lack a quantitative measure of the spatial  
 1036 | distribution of clast imbrications and clast arrangements, [\(Bertin and Friedrich, 2018\)](#). In the  
 1037 | same sense, the hydrologic calculations and force balancing approaches are based on the  
 1038 | simplest published expressions where water flow is related to sediment transport. Larger  
 1039 | complexities, which complicate any considerations of material transport (Engelund and  
 1040 | Hansen, 1967), have not been considered. This includes, for instance, large supply rates  
 1041 | of sediment [\(van der Berg and Schlunegger, 2012; Bekaddour et al., 2013\)](#), changes in  
 1042 | bed morphology, spatial variations in turbulences, the shape and the sorting of grains, [the](#)  
 1043 | [3D arrangement of clasts \(Lamb et al., 2008; Hodge et al., 2009\), and more complex](#)  
 1044 | [hydrological conditions including upper-stage plain beds, hydraulic drops, and standing](#)  
 1045 | [waves \(Johansson, 1963\). In addition, the occurrence or absence of imbrications also](#)  
 1046 | [strongly depends on the shape of the involved clasts \(Carling et al., 1992\). In particular,](#)

- geo Uni Bern 30.7.2018 22:11  
**Deleted:** also supported by
- geo Uni Bern 30.7.2018 22:11  
**Moved (insertion) [2]**
- geo Uni Bern 30.7.2018 22:11  
**Formatted:** English (US), Pattern: Clear
- geo Uni Bern 30.7.2018 22:11  
**Moved (insertion) [3]**
- geo Uni Bern 30.7.2018 22:11  
**Formatted:** English (US), Pattern: Clear
- geo Uni Bern 30.7.2018 22:11  
**Formatted:** Not Expanded by / Condensed by
- geo Uni Bern 30.7.2018 22:11  
**Formatted:** English (US), Pattern: Clear
- geo Uni Bern 30.7.2018 22:11  
**Deleted:** However
- geo Uni Bern 30.7.2018 22:11  
**Deleted:** *Relationships between channel gradients, flow strengths and imbrication of clasts* ... [8]
- geo Uni Bern 30.7.2018 22:11  
**Moved up [2]:** 2008). In particular, Mueller et al. (2005) suggested that a
- geo Uni Bern 30.7.2018 22:11  
**Formatted:** English (US), Pattern: Clear
- geo Uni Bern 30.7.2018 22:11  
**Deleted:** ... [9]
- geo Uni Bern 30.7.2018 22:11  
**Formatted:** English (US), Pattern: Clear
- geo Uni Bern 30.7.2018 22:11  
**Deleted:**  $\phi$  value of c.
- geo Uni Bern 30.7.2018 22:11  
**Moved up [3]:** 0.03 is suitable for slopes  $<0.35^\circ$ , while  $\phi > 0.1$  might be more appropriate for the mobilization of coarse-grained sediment particles in channels steeper than  $1.1^\circ$ .
- geo Uni Bern 30.7.2018 22:11  
**Formatted:** English (US), Pattern: Clear
- geo Uni Bern 30.7.2018 22:11  
**Formatted:** Not Expanded by / Condensed by
- geo Uni Bern 30.7.2018 22:11  
**Deleted:** is
- geo Uni Bern 30.7.2018 22:11  
**Deleted:** , or at least for changes from upper to lower flow regimes
- geo Uni Bern 30.7.2018 22:11  
**Deleted:** °.
- geo Uni Bern 30.7.2018 22:11  
**Deleted:** .
- geo Uni Bern 30.7.2018 22:11  
**Deleted:** taken
- geo Uni Bern 30.7.2018 22:11  
**Deleted:** and the 3D arrangement of clasts (Lamb et al., 2008). Despite our simplifications, we do find evidence ... [10]

1097 clasts with a relatively large c-axis tend to form steeper imbrications compared to those  
1098 constituents where the c-axis is short. In addition, experimental results of Hattingh and  
1099 Illenberger (1995) showed that spheres and rods have a higher mobility than blades and  
1100 discs, which is explained by differences in the related lift and drag forces exerted on each  
1101 shape-type together with the angle of repose and pivotability of these shape types.  
1102 Unfortunately, we lack the quantitative dataset to properly address these points. We also  
1103 acknowledge that imbrications do form during subcritical flows in flume experiments at  
1104 conditions, which can be characterized by low  $\phi$ -values (Brayshaw, 1984; Carling et al.,  
1105 1992; Powell et al., 2016; Lamb et al., 2017). However, as already noted above, we find it  
1106 quite hard to upscale the experimental results (<20 meters) to the reach scale of our  
1107 observations where standing waves with wavelengths as long as 8 meters have been  
1108 observed (Figure 6B).

1109 Despite our simplifications, we find evidence for proposing that clast imbrications are likely  
1110 to be associated with supercritical flows provided that (i) channel gradients are steeper  
1111 than c.  $0.5^\circ \pm 0.1^\circ$ , and (ii) large clasts are tightly packed, closely arranged as cluster  
1112 bedforms and partly embedded in finer-grained sediment. Mobilization and  
1113 rearrangements of these structures require larger thresholds (Brayshaw, 1985), which  
1114 might be large enough ( $\phi$ -values possibly  $>0.05$ ) to allow supercritical conditions to occur.

1115 These findings might be useful for the quantification of hydrological conditions in coarse-  
1116 grained stratigraphic archives such as conglomerates. As a further implication, the  
1117 occurrence of imbrications in clastic sediments may be used to infer a minimum value of  
1118  $0.5^\circ \pm 0.1^\circ$  for the palaeo-topographic slope. Such a constraint might be beneficial for  
1119 palaeo-geographic reconstructions and for the analysis of a basin's subsidence history  
1120 through the back-stripping of strata (e.g., Schlunegger et al., 1997). Finally, for modern  
1121 streams, the presence of imbrications on gravel bars with closely packed clasts might be  
1122 more conclusive for inferring an upper flow regime upon material transport than other  
1123 bedforms such as transverse ribs or antidunes (Koster, 1978; Rust and Gostin, 1981),  
1124 mainly because clast imbrications have a better preservation potential and are easier to  
1125 recognize in the field.

1126

### 1127 Figure captions

1128 Figure 1: A) Photo showing hydraulic jump, and conceptualization of situation displayed  
1129 in photo of Figure 1A.  $F$ =Froude number;  $v$ =flow velocity,  $d$ =water depth. B)  
1130 Photo from Sense River, and cross-sections through reaches with upper and  
1131 lower flow regimes. Surface waves ( $\lambda \approx 20$ -30 cm) tend to fade out towards the  
1132 upstream direction relative to the flow movement where subcritical flows prevail  
1133 (section to the left). A hydraulic jump separates segments with a supercritical  
1134 flow from reaches with a subcritical flow where the bedrock builds a ramp. The

geo Uni Bern 30.7.2018 22:11

Deleted: paleo

geo Uni Bern 30.7.2018 22:11

Deleted: paleo

geo Uni Bern 30.7.2018 22:11

Deleted: clast

geo Uni Bern 30.7.2018 22:11

Deleted: . B) Conceptualization

1139 reach illustrated by the section to the right is characterized by standing waves  
1140 with wavelengths  $\lambda \approx 100$  cm. The dashed line illustrates the trace of the plane  
1141 that separates lower from upper regime flows. Please see Figure 2 for location  
1142 of photo.

1144 Figure 2: Sites where modern gravel bars in streams were inspected for the occurrence  
1145 of clast imbrications (blue dots). The figure also shows the locations of the  
1146 stratigraphic sections where conglomerates were analyzed for their  
1147 sedimentary structures. S=Sense; E=Emme; WE<sub>LIV</sub>=Waldemme,  
1148 WL=Waldemme at Littau, R=Reuss; L=Landquart; G=Glenner; M<sub>B</sub>, M<sub>V</sub>,  
1149 M<sub>L</sub>=Maggia at Bignasco, Visletto and Losone; V<sub>F</sub>, V<sub>M</sub>, V<sub>L</sub>=Verzasca at Frasco,  
1150 Motta and Lavertezzo. See Table 1 for coordinates of sites.

1151 The black squares are sites where Spreafico et al. (2001) have estimated  
1152 channel gradients and Froude numbers for low and high-stage flows. b=Birse-  
1153 Moutier, e=Emme-Burgdorf, g/=Glatt-Fällanden, g=Gürbe-Belp, m=Minster-  
1154 Euthal, /=Lütschine-Gsteig, s=Suze-Sonceboz, t=Thur-Stein

1156 Figure 3: Relationships between A) channel slope and Froude number  $F$ , and B) relative  
1157 bed roughness and  $F$ . These were calculated as a function of various Shields  
1158 (1936) variables  $\phi$ . The pale green field indicates the conditions where an  
1159 upper flow regime could prevail, while the yellow field delineates the  
1160 occurrence of lower flow regime conditions. In this context, we set the  
1161 threshold to a Froude number of c. 0.9. This is consistent with the estimation of  
1162 parameters for the formation of upper flow regime bedforms by Koster (1978).  
1163 Note that the bed roughness is the ratio between the  $D_{\beta 4}$  and the water depth  $d$   
1164 at the incipient motion of that particular size class. The vertical bars on Figure  
1165 3A also illustrate the Froude numbers that have been estimated by Spreafico  
1166 et al. (2001) for the following streams and locations: b=Birse-Moutier,  
1167 e=Emme-Burgdorf, g/=Glatt-Fällanden, g=Gürbe-Belp, m=Minster-Euthal,  
1168 /=Lütschine-Gsteig, s=Suze-Sonceboz, t=Thur-Stein. Please note that the low  
1169 values for the Thur and Birse Rivers might represent underestimates as these  
1170 streams show evidence for multiple hydraulic jumps during high stage flows.

1172 Figure 4: This figure relates the occurrence of imbrications (blue bars) or no imbrications  
1173 (red bars) to A) channel slopes and B) relative bed roughness. Red bars with  
1174 blue hatches indicate that imbrications have been found in places. Blue bars  
1175 with red hatches suggest that imbrications dominate the bar morphology, but  
1176 that reaches without imbrications are also present on the same gravel bar.  
1177 Data from modern streams are displayed above the horizontal axes, while

geo Uni Bern 30.7.2018 22:11  
Deleted: .

geo Uni Bern 30.7.2018 22:11  
Deleted: blue

geo Uni Bern 30.7.2018 22:11  
Deleted: red

geo Uni Bern 30.7.2018 22:11  
Formatted: Font color: Black

geo Uni Bern 30.7.2018 22:11  
Deleted: lower figures relate

geo Uni Bern 30.7.2018 22:11  
Deleted: C)

geo Uni Bern 30.7.2018 22:11  
Deleted: to

geo Uni Bern 30.7.2018 22:11  
Deleted: D).

1185 information from stratigraphic sections are placed below the slope and  
1186 roughness axes, respectively. S=Sense, S'=Sense with bedrock reach,  
1187 E=Emme, WE<sub>LIV</sub>=Waldemme, WL=Waldemme at Littau, R=Reuss;  
1188 L=Landquart; G=Glenner; M<sub>B</sub>, M<sub>V</sub>, M<sub>L</sub>=Maggia at Bignasco, Visletto and  
1189 Losone; V<sub>F</sub>, V<sub>M</sub>, V<sub>L</sub>=Verzasca at Frasco, Motta and Lavertezzo. See Table 1 for  
1190 coordinates of sites, and Figure 2 for locations where data were collected.

1191  
1192 Figure 5 A) Reuss River with evidence for standing waves along the thalweg. Othophoto  
1193 reproduced by permission of swisstopo (BA 18065). Please see Figure 2 for  
1194 location. B) Transverse and lateral bars in the Reuss River with imbricated  
1195 clasts on the lateral bar forming a riffle, and standing waves where the thalweg  
1196 crosses the riffle. The wavelength of the standing wave is c. 5 m. Arrow  
1197 indicates flow direction. Please see Figures 2 and 5A for location of photo.

1198  
1199 Figure 6: Photos from the field. A) Photo of subaquatic longitudinal bar taken along the  
1200 steep bedrock/gravel bar reach of the Sense River (see Figure 1B for location  
1201 of photo). The clasts in the foreground are clustered and imbricated, forming  
1202 the nucleus of a possible cluster bedform. This fabric most likely formed when  
1203 rolling clasts came to a halt behind the boulder at the front. The clasts in the  
1204 background are either flat lying or slightly imbricated. Except for a few sites,  
1205 nearly all grains are either partially buried by finer grained material or  
1206 interlocked by neighboring clasts. The overlying flow shows evidence for  
1207 supercritical conditions with standing waves. B) Standing waves with a  
1208 wavelength of c. 8 m in the Waldemme at Littau. Water fluxes are c. 100 m<sup>3</sup>/s.  
1209 Arrow indicates flow direction. C) Flat lying clasts on a lateral bar in the Sense  
1210 River. Arrow indicates clasts that are overlapping each other, resulting in a  
1211 shallow dip of <10° of the overriding clast. D) Imbricated clasts within the  
1212 Maggia River at Visletto. Arrow indicates flow direction. Please note that the  
1213 imbricated arrangements of clasts mainly include the largest constituents of the  
1214 gravel bar in the middle of the photo, and clasts of similar sizes. Therefore, for  
1215 this set of imbricated clasts, we do not consider that protrusion effects might  
1216 play a major role. See Figure 2 for location and Table 1 for coordinates.

1217  
1218 Figure 7: A) Conglomerates at Rigi with no evidence for clast imbrications. White lines  
1219 indicate the orientation of the bedding. B) Conglomerates at Rigi with  
1220 imbricated gravels to cobbles, that are arranged as cluster bedforms (C). Arrow  
1221 indicates paleoflow direction. White line refers to the bedding. Note that the  
1222 steep dip (>25°) of the a-b-planes of the imbricated clasts. See Figure 2 for  
1223 location and Table 1 for coordinates.

geo Uni Bern 30.7.2018 22:11  
Formatted: Font color: Black, Not Raised  
by / Lowered by

geo Uni Bern 30.7.2018 22:11  
Deleted: Figure 4: . Photos from the  
field. A

geo Uni Bern 30.7.2018 22:11  
Deleted: E

geo Uni Bern 30.7.2018 22:11  
Deleted: F

geo Uni Bern 30.7.2018 22:11  
Deleted: .

geo Uni Bern 30.7.2018 22:11  
Deleted: paleoflow

1230

1231 | Figure 8: Conceptual sketch illustrating the formation of an ensemble of imbricated  
1232 | clasts as time proceeds (A through C). According to this model, the site of  
1233 | sediment accumulation will migrate upstream.  $F$ =Froude number;  $v$ =flow  
1234 | velocity,  $d$ =water depth.

1235

1236 | Table 1: Grain size and observational data and that have been collected in the field.  
1237 | See text for further explanations.

1238

1239

#### 1240 Author contribution

1241 FS designed the study and carried out the calculations, PG and FS collected the data, FS  
1242 wrote the text with contributions by PG, both authors contributed to the analyses and  
1243 discussion of the results.

1244

#### 1245 Data availability

1246 | The authors declare they have no conflict of interest.

1247

#### 1248 Acknowledgements

1249 This research has been supported grant No 154198 awarded to Schlunegger by the Swiss  
1250 National Science Foundation.

1251

#### 1252 References

1253 | [Aberle, J., and Nikora, V., Statistical properties of armored gravel bed surfaces, Water  
1254 | Resour. Res., 42, W11414, 2006.](#)

1255 Allen, P.A., Earth Surface Processes, John Wiley and Sons, Oxford, 416 pp., 1997.

1256 Andrews, E.D., Bed-material entrainment and hydraulic geometry of gravel-bed rivers  
1257 in Colorado, GSA Bull., 95, 371-378, 1984.

1258 Alexander, J., Bridge, J.S., Cheel, R.J., and Leclair, S.F., Bedforms and associated  
1259 sedimentary structures formed under supercritical water flows over aggrading  
1260 sand beds, Sedimentology, 48, 133-152, 2001.

1261 Alexander, J., and Fielding, C., Gravel antidunes in the tropical Burdekin River,  
1262 Queensland, Australia, Sedimentology, 44, 327-337, 1997.

1263 | [Berther, R., Geomorphometrische Untersuchungen entlang der Entle, Ms. Thesis, Univ.  
1264 | Bern, Bern, Switzerland, 94 p., 2012.](#)

1265 | [Blissenbach, L., Relation of surface angle distribution to particle size distribution on  
1266 | alluvial fans, J. Sediment. Petrol., 22, 25-28, 1952.](#)

geo Uni Bern 30.7.2018 22:11

Deleted: 5

geo Uni Bern 30.7.2018 22:11

Deleted: proceeds

geo Uni Bern 30.7.2018 22:11

Deleted: The formation of such a sedimentary fabric requires that clasts are transported upon rolling. A hydraulic jump forms at the upstream end of the suite of imbricated clasts, because the flow on the stoss-side of the bedform most likely experiences a reduction of the flow velocity. This can then result in aggradation of clasts due to the drop of the shear stress.

geo Uni Bern 30.7.2018 22:11

Deleted: Figure 6: . A) Illustration of possible transport mechanisms of coarse grained bedload. The mobilization can be accomplished through sliding or rolling. Modified after Allen (1997). B) Forces operating on a clast upon sliding, and C) force balancing of a clast upon pivoting. See text for further information. - ... [11]

geo Uni Bern 30.7.2018 22:11

Deleted: Data

geo Uni Bern 30.7.2018 22:11

Deleted: has

geo Uni Bern 30.7.2018 22:11

Deleted: All data used in this publication are available. - ... [12]

geo Uni Bern 30.7.2018 22:11

Formatted: English (UK)

1294 Bekaddour, T., Schlunegger, F., Attal, M., and Norton, P.K., Lateral sediment sources  
1295 and knickzones as controls on spatio-temporal variations of sediment transport  
1296 in an Alpine river, *Sedimentology*, 60, 342-357, 2013.

1297 [Bray, D.I., and Church, M., Armored versus paved gravel beds. \*J. Hydraul. Div.\*, 106,  
1298 \*1937-1940\*, 1980.](#)

1299 [Buffington, J., Dietrich, W.E., and Kirchner, J.W., Friction angle measurements on a  
1300 naturally formed gravel streambed: Implications for critical boundary shear  
1301 stress, \*Water Res. Res.\*, 28, 411-425, 1992.](#)

1302 Buffington, J.M., and Montgomery, D. R., A systematic analysis of eight decades of  
1303 incipient motion studies, with special reference to gravel-bedded rivers, *Water  
1304 Resour. Res.*, 33, 1993-2029, 1997.

1305 [Bertin, S., and Friedrich, H., Effect of surface texture and structure on the development  
1306 of stable fluvial armors, \*Geomorphology\*, 306, 64-79, 2018.](#)

1307 [Brayshaw, A.C., Characteristics and origin of cluster bedforms in coarse-grained  
1308 alluvial channels, in: \*Sedimentology of Gravels and Conglomerates\*, edited by  
1309 \*Koster, E.H., and Steel, R.J., Mem. Can. Soc. Petrol. Geol.\*, 10, 77-85, 1984.,  
1310 \*1978\*.](#)

1311 [Brayshaw, A.C., Bed microtopography and entrainment thresholds in gravel-bed rivers,  
1312 \*GSA Bull.\*, 96, 218-223, 1985.](#)

1313 D'Arcy, M., Roda-Boluda, D.C., and Whittaker, A.C., Glacial-interglacial climate  
1314 changes recorded by debris flow fan deposits, Owens Valley, California, *Quat.  
1315 Sci. Rev.*, 169, 288-311, 2017.

1316 [Carling, P.A., Armored versus paved gravel beds – discussion. \*J. Hydraul. Div.\*, 107,  
1317 \*1117-1118\*, 1981.](#)

1318 [Carling, P.A., Kelsey, A., and Glaister, M.S., Effect of bed roughness, particle shape  
1319 and orientation on initial motion criteria, in: \*Dynamics of gravel-bed rivers\*,  
1320 edited by: \*Billi, P., Hey, R.D., Throne, C.R., and Tacconi, P.\*, 23-39. \*John Wiley  
1321 and Sons, Ltd., Chichester\*, 1992.](#)

1322 Church, M., Palaeohydrological reconstructions from a Holocene valley fill, *Fluvial  
1323 sedimentology*, edited by: *Miall, A.D.*, *Mem. Can. Soc. Petrol. Geol.*, 5, 743-772,  
1324 1978.

1325 [Church, M., Bed material transport and the morphology of alluvial river channels, \*Ann.  
1326 Rev. Earth Planet. Sci.\*, 34, 325–354, 2006.](#)

1327 Department of Mines and Technology Surveys, Atlas of Canada, Geogr. Branch,  
1328 Ottawa, 1957.

1329 Duller, R.A., Whittaker, A.C., Swinehart, J.B., Armitage, J.J., Sinclair, H.D., Bair, A.,  
1330 and Allen, P.A., Abrupt landscape change post-6Ma on the central Great Plains,  
1331 USA, *Geology*, 40, 871-874, 2012.

1332 Engesser, B., and Kälin, D., *Eomys helveticus* n. sp. and *Eomys schluneggeri* n. sp.,  
1333 two new small eomyids of the Chattian (MP 25/MP 26) subalpine Lower  
1334 Freshwater Molasse of Switzerland, Fossil Imprint, 73, 213–224, 2017.

1335 Englund, F., and Hansen, E., A monograph on sediment transport in alluvial streams,  
1336 Teknisk Forlag – Copenhagen, 62 pp., 1967.

1337 Ferguson, R., Flow resistance equations for gravel- and boulder- bed streams. *Water*  
1338 *Resour. Res.*, 43, W05427, 2007.

1339 [Ferguson, R., River channel slope, flow resistance, and gravel entrainment thresholds,](#)  
1340 [Water Resour. Res.](#), 48, W05517, doi:10.1029/2011WR010850, 2012.

1341 Garefalakis, P., and Schlunegger, F., Link between concentrations of sediment flux and  
1342 deep crustal processes beneath the European Alps, *Sci. Rep.*, 8, 183,  
1343 doi:10.1038/s41598-017-17182-8

1344 Grant, G.E., Swanson, F.J., and Wolman, M.G., Pattern and origin of stepped-bed  
1345 morphology in high gradient streams, western Cascades, Oregon, *GSA Bull.*, 102,  
1346 340–352, 1990.

1347 Grant, G.E., Critical flow constrains flow hydraulics in mobile-bed streams: A new  
1348 hypothesis, *Water Resour. Res.*, 33, 349-358, 1997.

1349 [Haynes, H., and Pender, G., Stress history effects on graded bed stability, J. Hydraul.](#)  
1350 [Eng.](#), 33, 343-349, 2007.

1351 [Hattingh, J., and Illenberger, W.K., Shape sorting of flood-transported synthetic clasts](#)  
1352 [in a gravel bed river, Sed. Geol.](#), 96, 181-190, 1995.

1353 Hey, R.D., and Thorne, C.R., Stable channels with mobile gravel beds, *J. Hydr. Eng.*,  
1354 112, 671-689, 1986.

1355 [Hodge, R., Brasington, J., and Richards, K., In situ characterization of grain-scale](#)  
1356 [fluvial morphology using Terrestrial Laser Scanning, Earth Surf. Process.](#)  
1357 [Landf.](#), 34, 954-968, 2009.

1358 Howard, A.D., in: *Thresholds in Geomorphology*, edited by: Coates, D.R., and Vitek,  
1359 J.D., Allen and Unwin, Boston, MA, 227-258, 1980.

1360 Jarrett, R.D., Hydraulics of high-gradient streams. *J. Hydr. Eng.*, 110, 1519-1939,  
1361 1984.

1362 [Johansson, C.E., Orientation of pebbles in running water: a laboratory study, Geogr.](#)  
1363 [Ann.](#), 45, 85-112, 1963.

1364 [Johnston, C.E., Andrews, E.D., and Pitlick, J., In situ determination of particle friction](#)  
1365 [angles of fluvial gravels, Water Resour. Res.](#), 34, 2017-2030, 1998.

1366 Kempf, O., Matter, A., Burbank, D.W., and Mange, M., Depositional and structural  
1367 evolution of a foreland basin margin in a magnetostratigraphic framework; the  
1368 eastern Swiss Molasse Basin, *Int. J. Earth Sci.*, 88, 253–275, 1999.

geo Uni Bern 30.7.2018 22:11  
Formatted: English (UK)

geo Uni Bern 30.7.2018 22:11  
Formatted: Justified

geo Uni Bern 30.7.2018 22:11  
Formatted: Justified

geo Uni Bern 30.7.2018 22:11  
Formatted: English (UK)

1369 [Kirchner, J.W., Dietrich, W.E., Iseya, F., and Ikeda, H., The variability of critical shear](#)  
 1370 [stress, friction angle, and grain protrusion in water-worked sediments,](#)  
 1371 [Sedimentology, 37, 647-672, 1990.](#)

1372 Koster, E.H., Transverse ribs: their characteristics, origin and paleohydraulic  
 1373 significance, in: Fluvial sedimentology, edited by: Miall, A.D., Mem. Can. Soc.  
 1374 Petrol. Geol., 5, 161-186, 1978.

1375 Krogstad, P.A., and Antonia, R.A., Surface roughness effects in turbulent boundary  
 1376 layers, Exp. Fluids, 27, 450-460, 1999.

1377 [Lamb, M.P., Dietrich, W.E., and Venditti, J.G., Is the critical Shields stress for incipient](#)  
 1378 [sediment motion dependent on channel bed slope?, J. Geophys. Res., 113,](#)  
 1379 [F02008, 2008.](#)

1380 [Lamb, M.P., Brun, F., and Fuller, B.M., Hydrodynamics of steep streams with planar](#)  
 1381 [coarse-grained beds: Turbulence, flow resistance, and implications for sediment](#)  
 1382 [transport, Water Resour. Res., 53, 2240-2263, 2017.](#)

1383 [Lenzi, M.A., Mao, I., and Comiti, F., When does bedload transport begin in steep](#)  
 1384 [boulder-bed streams?, Hydrol. Proc., 20, 3517-3533, 2006.](#)

1385 [Li, Z., and Komar, P.D., Laboratory measurements of pivoting angles for applications to](#)  
 1386 [selective entrainment of gravel in a current, Sedimentology, 33, 413-423, 1986.](#)

1387 Litty, C., and Schlunegger, F., Controls on pebbles' size and shapes in streams off the  
 1388 Swiss Alps, J. Geol., 123, 405-427, 2017.

1389 [Matter, A.: Sedimentologische Untersuchungen im östlichen Napfgebiet \(Entlebuch –](#)  
 1390 [Tal der Grossen Fontanne, Kt. Luzern\), Eclogae Geol. Helv., 57, 315-428, 1964.](#)

1391 McDonald, B.C., and Banerjee, I., Sediments and bedforms on a braided outwash plain,  
 1392 Can. J. Earth Sci., 8, 1282-1301, 1971.

1393 Meyer-Peter, E., and Müller, R., Formulas for bedload transport, Proceedings of the 2<sup>nd</sup>  
 1394 meeting of the Int. Assoc. Hydraul. Struct. Res., Stockholm, Sweden. Appendix 2,  
 1395 39-64, 1948.

1396 Miall, A.D., Fluvial sedimentology: An historical overview, in: Fluvial sedimentology,  
 1397 edited by: Miall, A.D., Mem. Can. Soc. Petrol. Geol., 5, 1-48, 1978.

1398 Middleton, L.T., and Trujillo, A.P., Sedimentology and depositional setting of the upper  
 1399 Proterozoic Scanlan Conglomerate, central Arizona. In: Sedimentology of  
 1400 gravels and conglomerates, edited by: Koster, E.H., and Steel, R.J., Mem. Can.  
 1401 Soc. Petrol. Geol., 10, 189-202, 1984.

1402 Mueller, E.R., Pitlick, J., and Nelson, J.M., Variation in the reference Shields stress for  
 1403 bed load transport in gravel-bed streams and rivers, Water Resour. Res., 41,  
 1404 W04006, 2005.

1405 [Ockleford, A.-M., and Haynes, H., The impact of stress history on bed structure, Earth](#)  
 1406 [Surf. Process. Landf., 38, 717-727, 2013.](#)

geo Uni Bern 30.7.2018 22:11

**Deleted:** Komar, P.D., Entrainment of sediments from deposits of mixed grain sizes and densities, in: advances in fluvial dynamics and stratigraphy, edited by Carling, P.A., and Dawson, M.R., John Wiley and Sons, Chichester, 127-181, 1996. -

geo Uni Bern 30.7.2018 22:11

**Formatted:** English (UK)

geo Uni Bern 30.7.2018 22:11

**Deleted:** Ist he

geo Uni Bern 30.7.2018 22:11

**Formatted:** English (UK)

geo Uni Bern 30.7.2018 22:11

**Formatted:** English (UK)

geo Uni Bern 30.7.2018 22:11

**Formatted:** German (Switzerland)



- 1415 Papaevangelou, G., Evangelides, C., and Tsimopoulos, C., A new explicit relation for  
1416 friction coefficient  $f$  in the Darcy-Weisbach equation, Proc. 10<sup>th</sup> Conf. Prot.  
1417 Restor. Env., PRE10, July 6-9, 2010.
- 1418 Paola, C., Heller, P.L., and Angevine, C., The large-scale dynamics of grain-size  
1419 variation in alluvial basins, 1: Theory, Basin Res., 4, 73-90, 1992.
- 1420 Paola, C., and Mohring, D., Palaeohydraulics revisited: palaeoslope estimation in  
1421 coarse-grained braided rivers. Basin Res., 8, 243-254, 1996.
- 1422 [Parker, G., Self-formed straight rivers with equilibrium banks and mobile bed. Part 2.](#)  
1423 [The gravel river, J. Fluid Mech., 89, 127-146, 1978.](#)  
1424 [doi:10.1017/S002112078002505.](#)
- 1425 Pettijohn, F.J., Sedimentary rocks, Harper and Brothers, New York, 718 pp., 1957.
- 1426 [Pfeiffer, A.M., Finnegan, N.J., and Willenbring, J.K., Sediment supply controls](#)  
1427 [equilibrium channel geometry in gravel rivers, Proc. Natl. Acad. Sci. U.S.A.,](#)  
1428 [114, 3346-3351, 2017.](#)
- 1429 [Philips, C.B., and Jerolmack, D.J., Self-organization of river channels as a critical filter](#)  
1430 [on climate signals, Science, 352, 649-697, 2016.](#)
- 1431 Potsma, G., and Roep, T., Resedimented conglomerates in the bottomsets of Gilbert-  
1432 type gravel deltas, J. Sed. Petrol., 55, 874-885, 1985.
- 1433 [Powell, M.D., Ockleford, A., Rice, S.P., Hillier, J.K., Nguyen, T., Reid, I., Tate, N.J.,](#)  
1434 [and Ackerley, D., Structural properties of mobile armors formed at different flow](#)  
1435 [strengths in gravel-bed rivers. J. Geophys. Res. – Earth Surface, 121, 1494-](#)  
1436 [1515, 2016.](#)
- 1437 [Qin, J., Zhong, D., Wang, G., and Ng, S.L., Influence of particle shape on surface](#)  
1438 [roughness: Dissimilar morphological structures formed by man-made and](#)  
1439 [natural gravels, Geomorphology, 190, 16-26, 2013.](#)
- 1440 Rust, B.R., Depositional models for braided alluvium, in: Fluvial sedimentology, edited  
1441 by: Miall, A.D., Mem. Can. Soc. Petrol. Geol., 5, 221-245, 1978.
- 1442 Rust, B.R., Proximal braidplain deposits in the Middle Devonian Malbaie Formation of  
1443 eastern Gaspé, Quebec, Canada, Sedimentology, 31, 675-695, 1984.
- 1444 Rust, B.R., and Gostin, V.A., Fossil transverse ribs in Holocene alluvial fan deposits,  
1445 Depot Creek, South Australia, J. Sediment. Petrol., 51, 441-444, 1981.
- 1446 [Sengupta, S., Studies on orientation and imbrication of pebbles with respect to cross-](#)  
1447 [stratification, J. Sed. Petrol., 36, 227-237, 1966.](#)
- 1448 Shao, Z., Zhong, J., Li, Y., Mao, C., Liu, S., Ni, L., Tian, Y., Cui, X., Liu, Y., Wang, X.,  
1449 Li, W., and Lin, G., Characteristics and sedimentary processes of lamina-  
1450 controlled sand-particle imbricate structure in deposits of Lingshan Island,  
1451 Qingdao, China, Sci. China Earth Sci., 57, 1061-1076, 2014.
- 1452 Schlunegger, F., Burbank, D.W., Matter, A., Engesser, B., and Mödden, C.,  
1453 Magnetostratigraphic calibration of the Oligocene to Middle Miocene (30-15 Ma)

- 1454 mammal bizonas and depositional sequences of the central Swiss Molasse  
1455 basin, *Eclogae geol. Helv.*, 89, 753-788, 1996.
- 1456 Schlunegger, F., Jordan, T.E., and Klaper, E.M., Controls of erosional denudation in  
1457 the orogeny on foreland basin evolution: The Oligocene central Swiss Molasse  
1458 Basin as an example, *Tectonics*, 16, 823-840, 1997.
- 1459 Schlunegger, F., and Norton, K.P., Climate vs. tectonics: the competing roles of Late  
1460 Oligocene warming and Alpine orogenesis in constructing alluvial megafan  
1461 sequences in the North Alpine foreland basin, *Basin Res.*, 27, 230-245, 2015.
- 1462 Schlunegger, F., Norton, K.P., Delunel, R., Ehlers, T.A., and Madella, A., Late Miocene  
1463 increase in precipitation in the Western Cordillera of the Andes between 18-19°  
1464 latitudes inferred from shifts in sedimentation patterns, *Earth Planet. Sci. Lett.*,  
1465 462, 157-168, 2017.
- 1466 [Schlunegger, F. and Castellort, S., Immediate and delayed signal of slab breakoff in  
1467 Oligo/Miocene Molasse deposits from the European Alps, \*Sci. Rep.\* 6, 31010,  
1468 2016.](#)
- 1469 Shaw, J., and Kellerhals, R., Paleohydraulic interpretation of antidune bedforms with  
1470 applications to antidunes in gravel, *J. Sediment. Petrol.*, 47, 257-266, 1977.
- 1471 Shields, A., Anwendungen der Aehnlichkeitsmechanik und der Turbulenzforschung  
1472 auf die Geschiebebewegung. *Mitt. Preuss. Versuch. Wasserbau Schiffbau*, 26,  
1473 Berlin, 1936.
- 1474 Simons, E.V., and Richardson, E.V., Discussion of resistance properties of sediment-  
1475 laden streams, *Am. Soc. Civil Eng. Trans.*, 125, 1170-1172, 1960.
- 1476 Sinclair, H.D., and Jaffey, N., Sedimentology of the Indus Group, Ladakh, northern  
1477 India: implications for the timing of initiation of the paeo-Indus River. *J. Geol.*  
1478 *Soc. London*, 158, 151-162, 2001.
- 1479 Slooman, A., Simpson, G., Castellort, S., and De Boer, P.L., Geological record of  
1480 marine tsunami backwash: The role of the hydraulic jump, *Depositional Record*,  
1481 1-19, 2018.
- 1482 [Spicher, A., Geologische Karte der Schweiz 1:500'000, Schweiz. Natf. Ges., 1980.](#)
- 1483 [Spreafico, M., Hodel, H.P., and Kaspar, H., Rauheiten in ausgesuchten  
1484 schweizerischen Fließgewässern, \*Berichte des BWG, Seri Wasser\*, 102 p.,  
1485 Bern, 2001.](#)
- 1486 Stürm, B., Die Rigischüttung. Sedimentpetrographie, Sedimentologie,  
1487 Paläogeographie, Tektonik, PhD thesis, Univ. Zürich, Switzerland, 98 p., 1973.
- 1488 [Van der Berg, F., and Schlunegger, F., Alluvial cover dynamics in response to floods of  
1489 various magnitudes: The effect of the release of glaciogenic material in a Swiss  
1490 Alpine catchment, \*Geomorphology\*, 141, 121-133, 2012.](#)
- 1491 [Wickert, A.D., and Schildgen, T.F., Long-profile evolution of transport-limited gravel-bed  
1492 rivers, \*Earth Surf. Dynam. Discuss.\*, doi: \[org/10.5194/esurf-2018-39\]\(https://doi.org/10.5194/esurf-2018-39\).](#)

geo Uni Bern 30.7.2018 22:11

Formatted: English (UK)

geo Uni Bern 30.7.2018 22:11

Formatted: German (Switzerland)

geo Uni Bern 30.7.2018 22:11

Formatted: German (Switzerland)

geo Uni Bern 30.7.2018 22:11

Formatted: English (UK)

1493 [Wong, M., and Parker, G., Reanalysis and correction of bed-load relation of Meyer-](#)  
1494 [Peter and Müller using their own database, J. Hydraul. Eng., 132, 1159-1168,](#)  
1495 [2006.](#)

1496 [Taki, K., and Parker, G., Transportational cyclic steps cre-](#) ated by flow over an erodible  
1497 bed. Part 1. Experiments, J. Hydrol. Res., 43, 488–501, 2005.

1498 Todd, S.P., Process deduction from fluvial sedimentary structures, in: Advances in  
1499 fluvial dynamics and stratigraphy, edited by: Carling, P.A., and Dawson, M.R.,  
1500 John Wiley & Sons Ltd, 299-350, 1996.

1501 Trieste, D.J., Evaluation of supercritical/subcritical flows in high-gradient channel, J.  
1502 Hydr. Eng., 118, 1107-1118, 1992.

1503 Trieste, D.J., Supercritical flows versus subcritical flows in natural channels, in:  
1504 Hydraulic Engineering '94: Proceedings of the 1994 Conference of the  
1505 Hydraulics Division, edited by: Cotroneo, G.V., and Rumer, R.R., Am. Soc. Civ.  
1506 Eng., New York, 732-736, 1994.

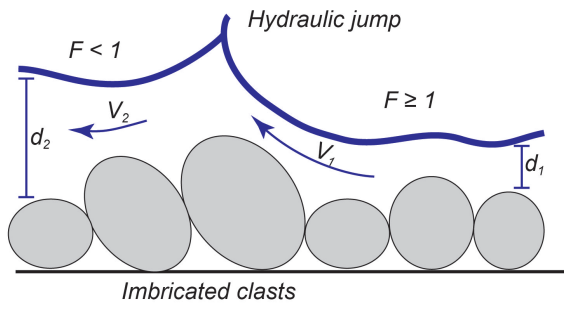
1507 Tucker, G., and Slingerland, R., Drainage basin responses to climate change, Water  
1508 Resour. Res., 33, 2031-2047, 1997.

1509 Whipple, K.X., Bedrock rivers and the geomorphology of active orogens, Ann. Rev. Earth  
1510 Planet. Sci., 32, 151–185, 2004.

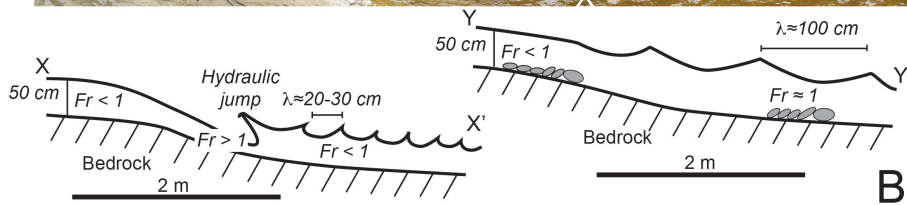
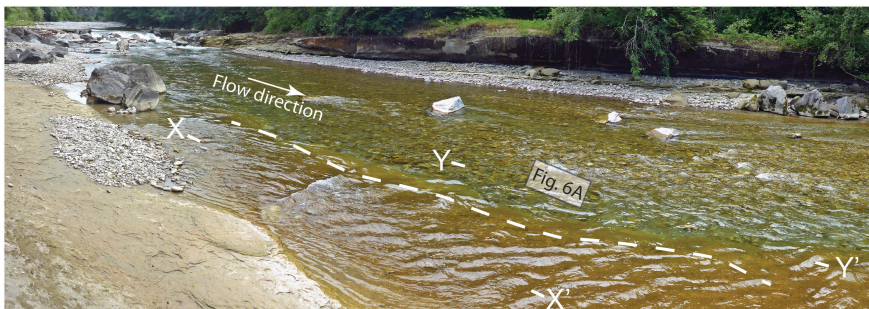
1511 Wiberg, P.L., and Smith, J.D., Velocity distribution and bed roughness in high-gradient  
1512 streams, Water Resour. Res., 27, 825-838, 1991.

1513 Yagishita, K., Paleocurrent and fabric analyses of fluvial conglomerates of the  
1514 Paeogene Noda Group, northeast Japan, Sed. Geol., 109, 53-71, 1997.

1515



A



B

Figure 1

1516  
1517

Figure 1

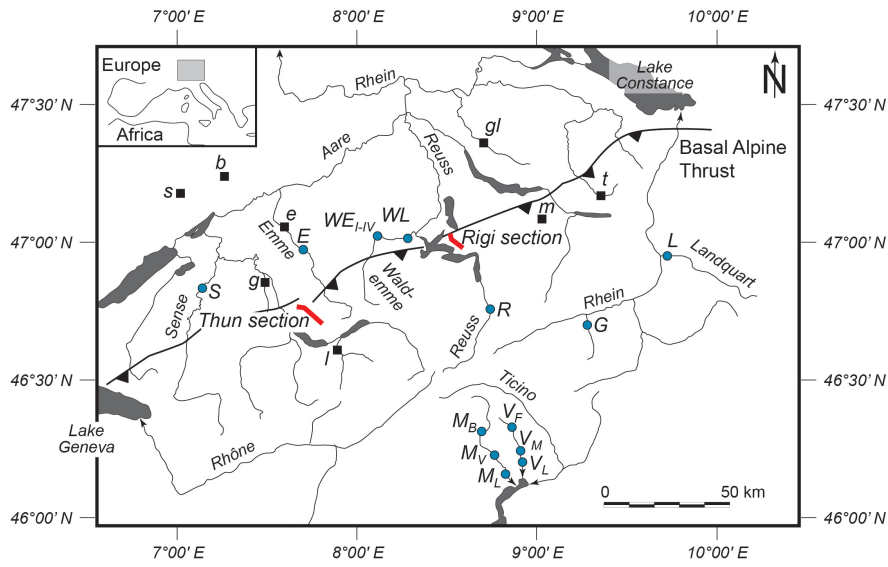


Figure 2

1522

1523 Figure 2

1524

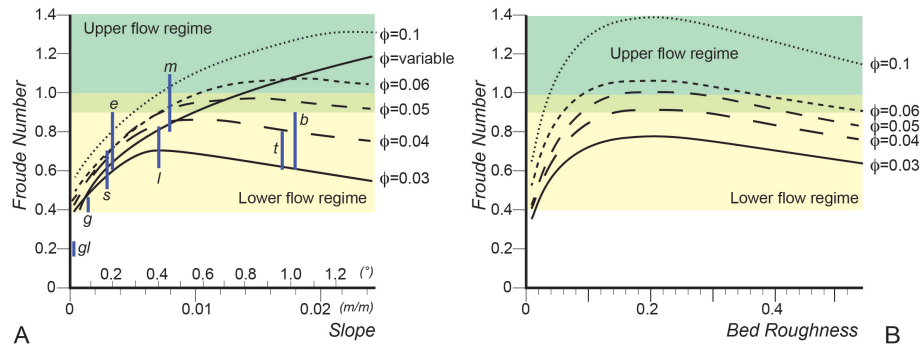
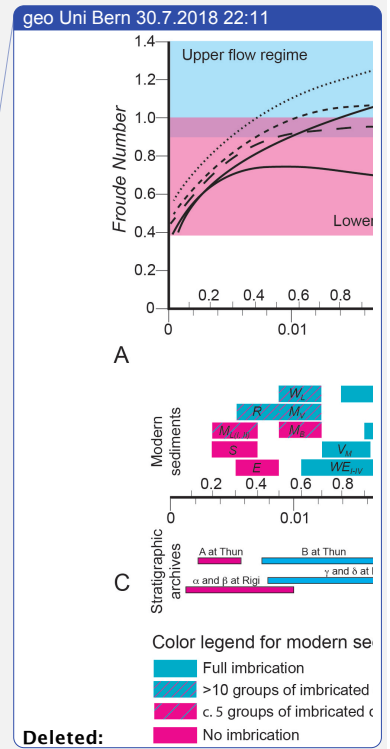


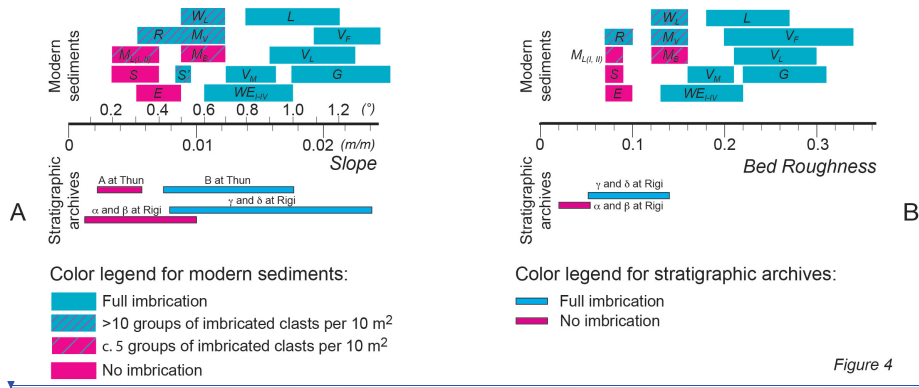
Figure 3

1528

1529 Figure 3

1530

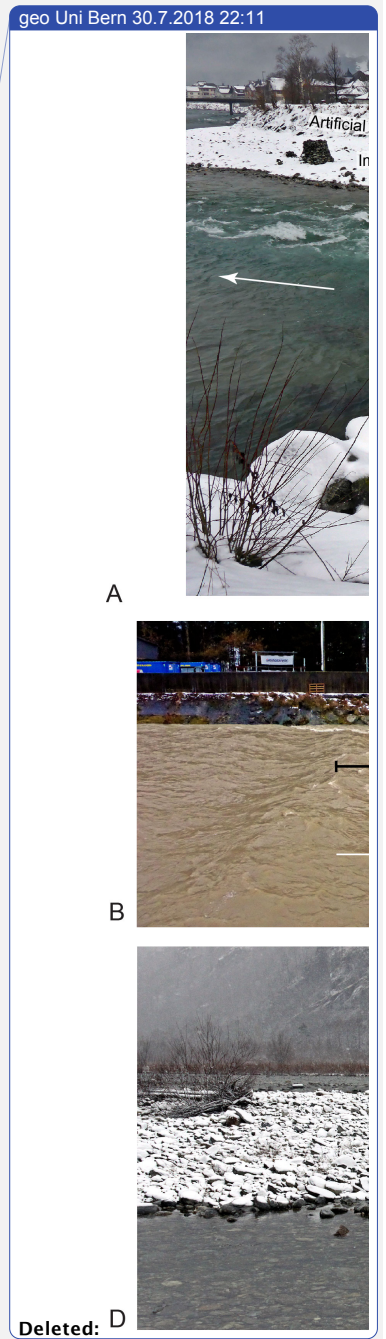


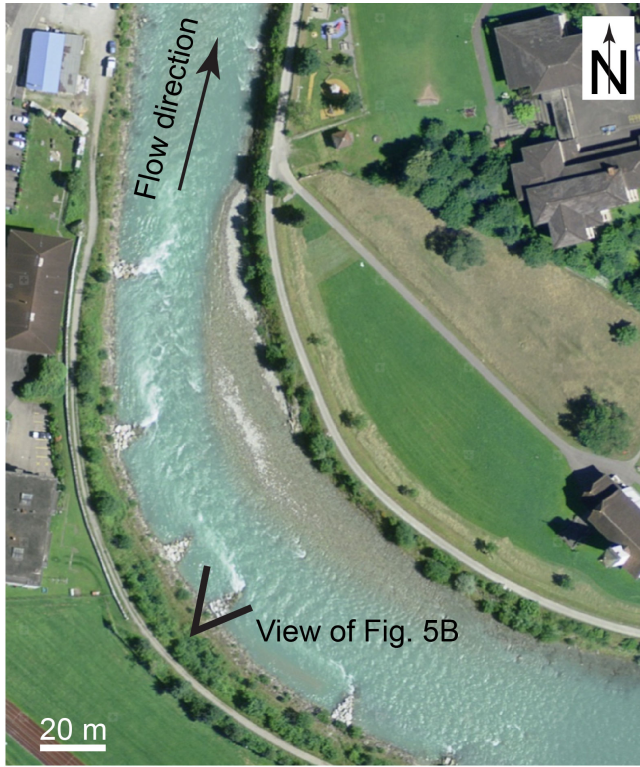


1532

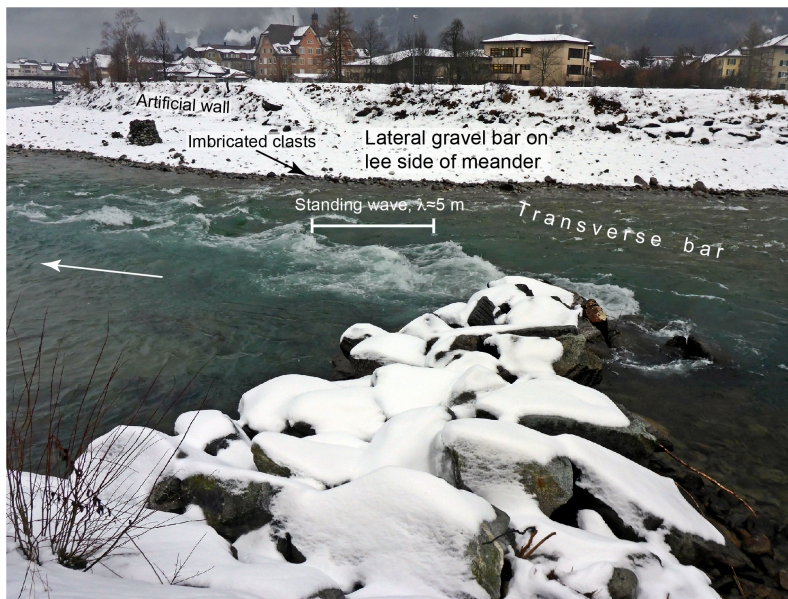
1533 **Figure 4**

1534

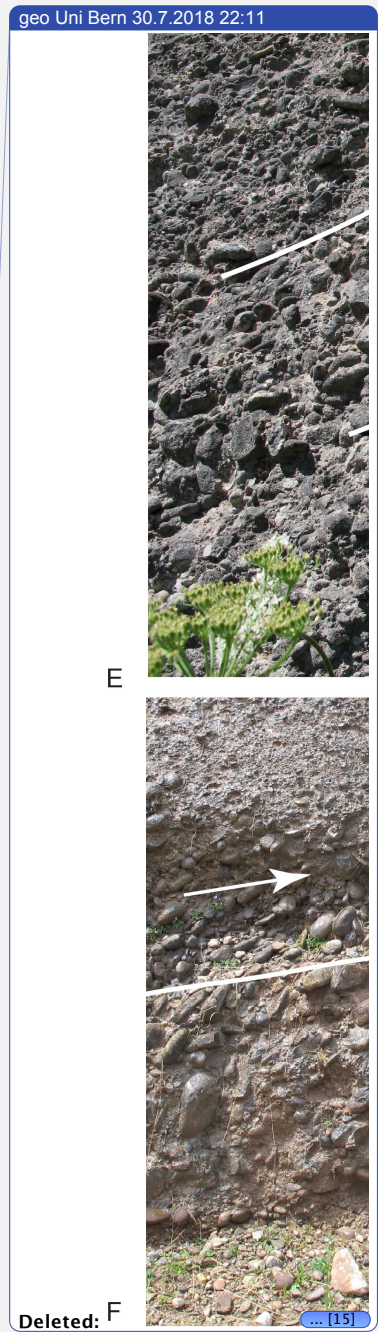




A



B



E

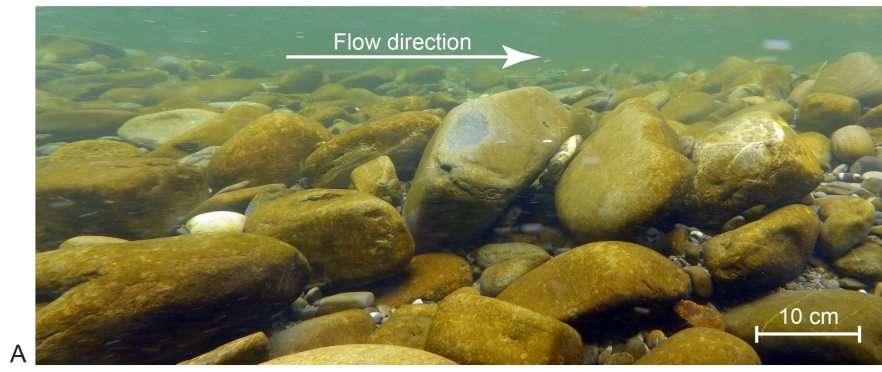
Deleted: F

1536

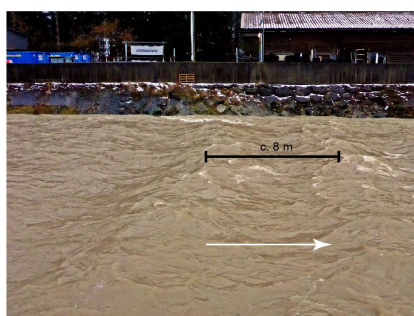
1537 Figure 5

1538





A



B



C

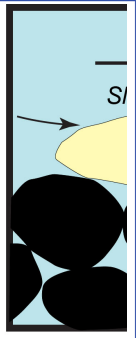


D

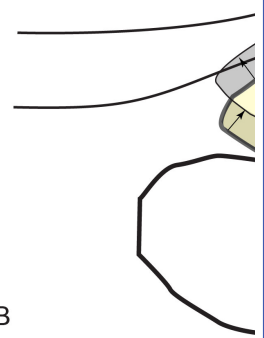
Figure 6

1541  
1542  
1543

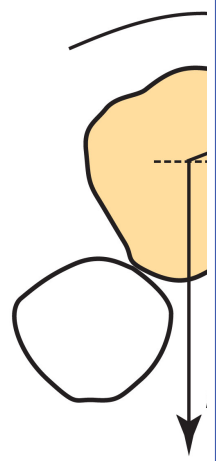
Figure 6



A

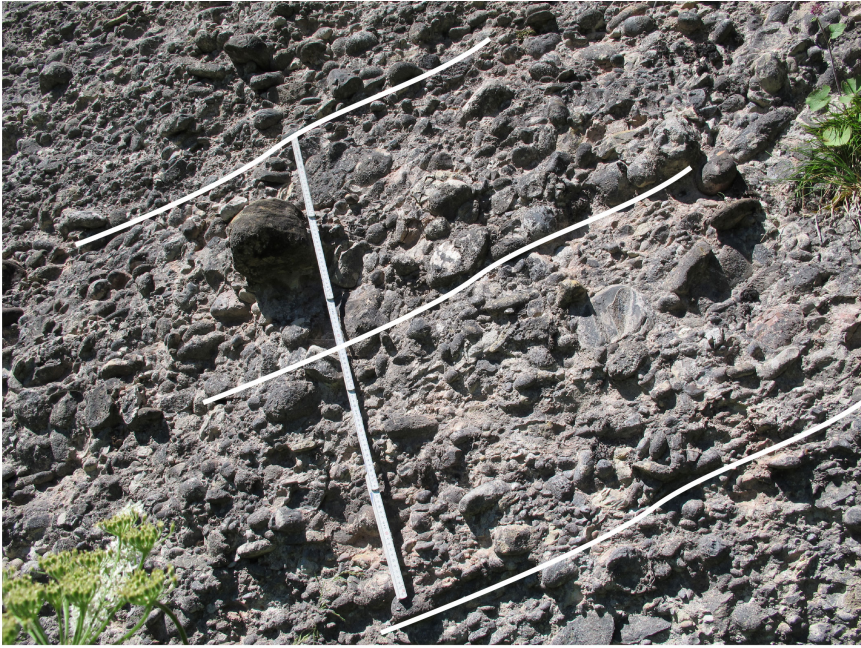


B

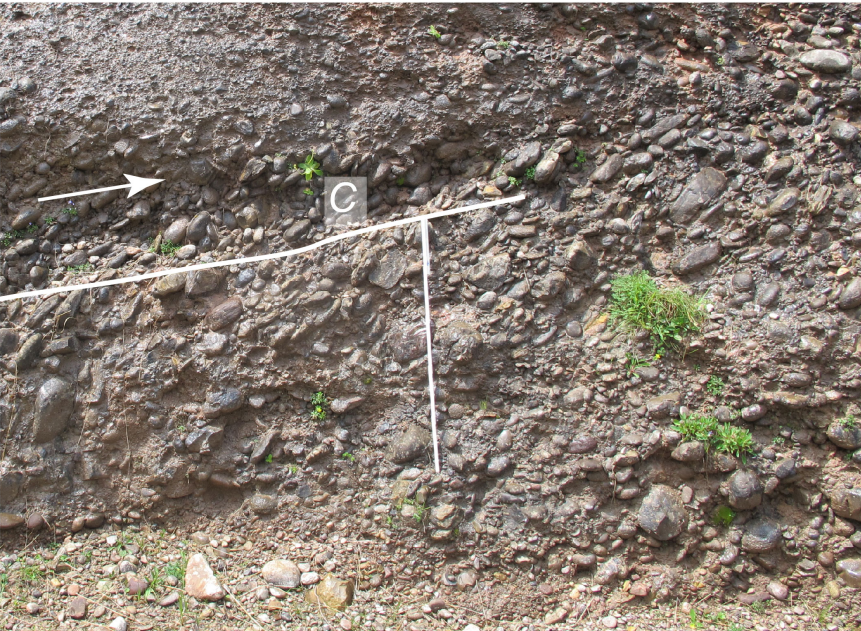


C

Deleted:  
geo Uni Bern 30.7.2018 22:11  
Formatted: Font:11 pt  
geo Uni Bern 30.7.2018 22:11  
Deleted: -



A



B

1546

1547

1548

Figure 7

[Figure 7](#)

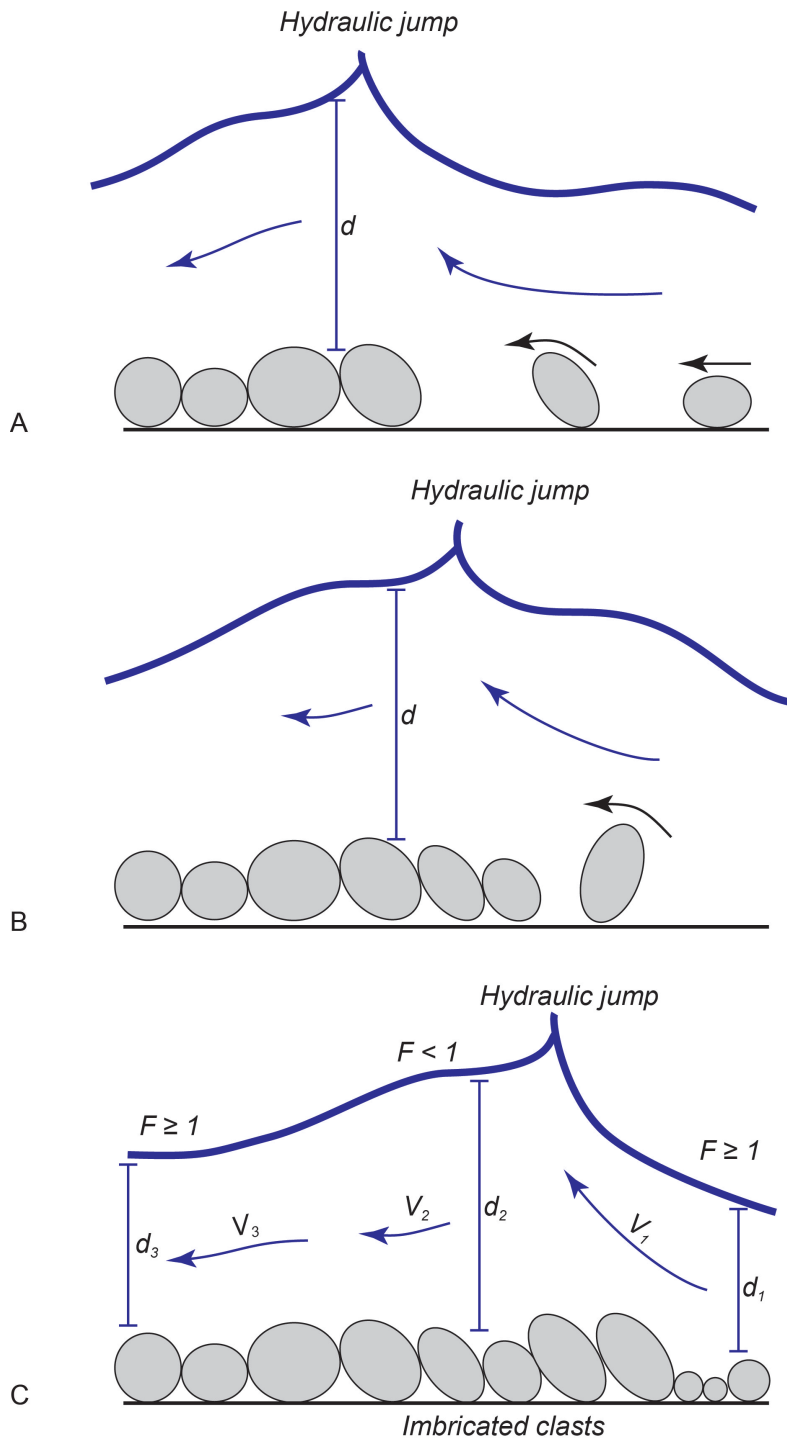


Figure 8

1549  
1550

Figure 8

**Modern gravel bars**

Site name	Abbreviation	Site coordinates	D84 (cm)	D50 (cm)	D84/D50	D96 (cm)	Gradient (m/m)	Gradient (°)	Inferred water depth d (m)	Roughness	Imbrication
Emme	E	46°57'08N / 7°44'59E	2.3	0.9	2.56	5.2	0.005-0.008	0.4±0.1	0.5-0.8	0.07-0.10	mostly no
	G	46°44'42N / 9°13'04E	12	2.88	4.17	27.4	0.017-0.024	1.2±0.2	0.4-0.6	0.22-0.31	mostly yes; largest boulders imbricated; smaller pebbles deposited in-between without preferred orientation, sand covers the clast fabric
Landquart	L	46°57'08N / 7°44'59E	10	2.5	4.00	13.5	0.014-0.021	1.0±0.2	0.4-0.6	0.18-0.27	yes
	Maggia Bignasco	MB	46°44'42N / 9°13'04E	2.7	0.85	3.18	13	0.009-0.012	0.6±0.1	0.2	0.12-0.16
Maggia Viletto	MV	46°58'26N / 9°36'29E	9.5	2.29	4.15	20	0.009-0.012	0.6±0.1	0.3-0.5	0.12-0.16	partly yes
	Maggia Losone I	ML I	46°20'08N / 8°36'25E	4	0.79	5.06	14	0.005-0.007	0.3±0.1	0.5-0.6	0.07-0.09
Maggia Losone II	ML II	46°18'30N / 8°36'35E	6	1.12	5.36	12.65	0.005-0.007	0.3±0.1	0.7-1.0	0.07-0.09	triplets and quadruplets of imbricated clasts occur in places
Verzasca Frasco	VF	46°10'46N / 8°45'33E	2.5	0.75	3.33	7	0.015-0.026	1.3±0.2	0.1	0.20-0.34	imbricated
Verzasca Molta	VM	46°10'15N / 8°46'10E	4.3	1.44	2.99	18.75	0.012-0.016	0.9±0.2	0.2-0.3	0.18-0.21	largest boulders imbricated smaller pebbles deposited in-between without preferred orientation, finer-grained bedforms show imbricated clasts where no boulders are present
Verzasca Lavartezzo	LV	46°20'20N / 8°48'03E	5	1.3	3.85	30	0.016-0.023	1.1±0.2	0.2-0.3	0.21-0.30	largest boulders imbricated smaller pebbles deposited in-between without preferred orientation as inferred from photos
Reuss		46°16'28N / 8°48'34E	3.2	0.88	3.64	6.37	0.005-0.008	0.4±0.1	0.3-0.5	0.07-0.10	to large extents yes, triplets and quadruplets of imbricated clasts occur in places. Stream shows standing waves and hydraulic jumps in steep reaches and lower flow regime conditions in flat segments
Sense		46°15'21N / 8°50'23E	6	2.42	2.48	9.58	0.005-0.007	0.3±0.1	0.7-1.0	0.07-0.09	mostly no; imbrications only at the steep, downstream slip-faces of transverse bars
Waldemme Littau	WL	46°48'53N / 8°39'16E	3.5	0.9	3.89	8.36	0.009-0.012	0.6±0.1	0.2-0.3	0.12-0.16	triplets and quadruplets of imbricated clasts occur in places
Waldemme Entlebuch I	WE I	46°53'20N / 7°20'56E	3	1	3.00	9	0.01-0.017	0.8±0.2	0.1-0.2	0.13-0.22	yes
Waldemme Entlebuch II	WE II	47°03'04N / 8°15'13E	8	2.43	3.29	18	0.01-0.017	0.8±0.2	0.4-0.6	0.13-0.22	yes
Waldemme Entlebuch III	WE III	47°01'57N / 8°04'03E	6.7	2.57	2.22	14	0.01-0.017	0.8±0.2	0.3-0.5	0.13-0.22	yes
Waldemme Entlebuch IV	WE IV	47°01'57N / 8°04'03E	8.2	2.68	3.06	18	0.01-0.017	0.8±0.2	0.4-0.7	0.13-0.22	yes

**Stratigraphic archives**

Rigi conglomerates						
Segment	D84 (m)	Slope (m/m)	Slope (°)	Inferred water depth d (m)	D84/d	Imbrication
β	0.07-0.12	0.008-0.027	0.9±0.4	1.2±0.35	0.05-0.14	yes, in places
γ	0.06-0.1	0.008-0.015	0.65±0.2	1.2±0.4	0.04-0.12	partly yes
β	0.04-0.06	0.005-0.01	0.4±0.2	1.7±0.5	0.02-0.05	no
α	0.04-0.06	0.002-0.005	0.2±0.06	2.5±0.8	0.02-0.04	no

Thun conglomerates						
Unit	D84 (m)	Slope (m/m)	Slope (°)	Inferred water depth d (m)	D84/d	Imbrication
B	not available	0.008-0.017	0.72±0.3	1.5-3	not available	yes, in places
A	not available	0.003-0.005	0.23±0.1	3-5	not available	no

1551

1552

1553

Table 1